Renewable and Sustainable Energy Reviews 157 (2022) 112056

Contents lists available at ScienceDirect

Renewable and Sustainable Energy Reviews

journal homepage: www.elsevier.com/locate/rser

Lignocellulosic biomass carbonization for biochar production and characterization of biochar reactivity

Fanzhi Qin [a,b], Chen Zhang [a,b,*], Guangming Zeng [a,b], Danlian Huang [a,b], Xiaofei Tan [a,b], Abing Duan [a,b]

[a] College of Environmental Science and Engineering, Hunan University, Changsha, 410082, PR China
[b] Key Laboratory of Environmental Biology and Pollution Control, Ministry of Education, Hunan University, Changsha, 410082, PR China

ARTICLE INFO

Keywords:
Lignocellulosic biomass
Carbonization
Biochar
Reactivity
Sustainable conversion technologies

ABSTRACT

Lignocellulosic biomass (LB) pyrolysis and gasification technologies for bio-oil, syngas and process heat have been widely described, and biochar, as a significant byproduct of LB pyrolysis, has also received increasing attention because of it global sustainability. Biochar is attractive to researchers, mainly due to the value of its activity and reactivity, bringing the possibility of achieving carbon utilization and carbon neutralization. However, few studies have systematically described the changes in chemical composition and structure of LB during its carbonization process, as well as the origin of produced biochar's reactivity. A better understanding of what chemical substances have facilitated biochar reactivity and how they function is needed, which is of great value for environmental remediation analysis and green application strategy formulation. Herein, the new insights into the possible decomposition/transformation mechanisms of LB to functionalized biochar were discussed. Subsequently, the basic structure of lignocellulosic biomass derived biochar (LBC) was studied, and its reactivity-related compositions were also summarized. More importantly, discussion was expanded on the origin of LBC's reactivity and the reactivity expression ways. And the outlook section will highlight insights into future directions and prospects, aiming to overcome current limitations by developing more methods and exploring other green applications.

1. Introduction

Excessive consumption of fossil fuels and its corresponding environment consequences have become global problems. In order to deal with increasingly severe global environmental rick, food security and energy shortage problems, it inevitably needs to seek innovation, efficient, sustainable and eco-feasible solutions [1–5]. Biomass is a typical sustainable bioresource, which refers to all kinds of organisms formed through photosynthesis using readily available carbon dioxide, water and sunlight in the atmosphere, including all animals, plants and microorganisms [6]. Compared with non-renewable fossil fuels, it is widely found in nature, possessing great prospects in producing energy, chemicals and other products [7–10]. The production of carbon-neutral materials (such as biochars [11] and carbon nanotubes [12]) and low-emission fuels [13–15] from this renewable resource is playing an increasingly important role in gradually replacing traditional fossil processes, and has received extensive attention from the academic field in the past decade [16].

Biochar (biomass-derived black carbon, BC) is defined as a kind of solid, highly aromatic and carbon-rich co-product produced by the heating process of biomass under oxygen-deficient or oxygen-free conditions [17]. It has inestimable potentials in agricultural production, energy storage, and environment management due to characteristics of high porosity, cation exchange capacity, absorbability, stability, nutrients and reactivity [18–20]. In energy storage, biochar can be designed as an electrode material for lithium ion batteries and supercapacitors, and as a catalyst for oxidation-reduction reaction and hydrogen storage process [19,21]. Also in environmental management, biochar can be used as an efficient amendment playing an important role in pollutants removing or stabilizing [22,23].

As a typical feedstock for biochar preparation, lignocellulosic biomass (LB) is the most abundant, cheapest and most widely sourced biomass on earth, which has been identified to be economically feasible and ecologically effective [7,24]. Compared with other biomass (*e.g.*, animal residues, food processing wastes, sewage sludges and municipal solid wastes), LB has the advantages of lower water content, less ash content, and simpler composition [25,26]. Meanwhile, the biochar

---

* Corresponding author. College of Environmental Science and Engineering, Hunan University, Changsha, 410082, PR China.
E-mail address: zhangchen@hnu.edu.cn (C. Zhang).

https://doi.org/10.1016/j.rser.2021.112056
Received 29 September 2021; Received in revised form 9 December 2021; Accepted 29 December 2021

List of abbreviations:

LB	Lignocellulosic biomass
LBC	Biochar derived from lignocellulosic biomass
LBCTs	LBC conversion technologies
OCs	Organic components
ICs	Inorganic components
MCs	Mineral compounds
FC	Fixed carbon
VMs	Volatile matters
HTC	Hydrothermal carbonization
BDE	Bond dissociation energies
DFT	Density functional theory
PPE	Phenylethyl phenyl ether
SSA	Specific surface area
ARS	Aromatic ring structure
CSS	Carbon skeleton structure
AFGs	Active functional groups
PFRs	Persistent free radicals
HMs	Heavy metals
NFGs	Nitrogen-containing functional groups
SFGs	Sulfur-containing functional groups
OFGs	Oxygen-containing functional groups
TMs	Transition metals
AOPs	Advanced oxidation processes
ROS	Reactive oxygen species

based on lignocellulosic biomass pyrolysis is significantly better than other sources in terms of pretreatment costs, surface structure advantages and application potentials. Table 1 summarizes the data on the current situation and application potentials of biochar production from different biomass in recent years. Hence, in industrial large-scale production, LB and its corresponding biochar has a higher practical value of popularization and application.

Biochar is attractive to researchers, mainly due to the value of its activity and reactivity, bringing the possibility of carbon utilization and carbon neutralization. In this study, we define the reactivity of biochar as the function of strengthening electron transfer and mediating chemical reaction promoted by special components or structures contained in biochar, which is different from its adsorption activity and conditioning effect (biochar activity). Although there are some literatures that have studied the influence of conditions in biochar preparation process and the effects of modification on biochar properties, the breakthrough points of paying attention to the reactivity exploration of biochar are not much. For example, Kan and his co-workers discussed the effects of pyrolysis parameters on the properties of LB products, but the viewpoint about changes of biochar characteristics was not given in essence [50]. While Mäkelä et al. studied the hydrothermal carbonization characteristics of LB, but did not pay more attention to the cause of rich active sites existing in biochar surface [26]. The studies on the reactivity of biochar derived from lignocellulosic biomass (LBC) are of great value because it can reveal how LBC is endowed with the ability of mediating electron transfer and promoting chemical reaction among substances, and can be used for reference to explore the reactivity of biochar conversion from other biomass [51]. And the exploration of its origin mechanism is also an important basis for environmental remediation analysis and green application strategy formulation based on efficient and sustainable biochar-based materials.

As a significant part of the biogeochemical carbon cycle, the efficient and sustainable utilization of biochar derived from LB is undoubtedly an essential means to deal with the global resource, energy and environment crisis. However, few studies have systematically described the changes in chemical composition and structure of LB during the biochar preparation process, as well as the origin of the reactivity of biochar. A better understanding of what chemical substances have facilitated biochar reactivity and how they origin is needed. Therefore, it is necessary to make an in-depth study on the conversion technology and reactivity of biochar derived from LB, which is of great value for achieving the goals about carbon cycle, carbon neutrality and global sustainable development.

Herein, this paper aims to provide the new insights into the possible mechanisms about decomposition/transformation of LB to functionalized biochar and LBC reactivity generation process at molecular level. Firstly, the latest achievements in sustainable LBC conversion technologies (LBCTs) have been summarized and the carbonization (biochar conversion) process of the main components of LB are clarified. Moreover, the difference and relationship between the product BC and the original LB in structure and reactivity-related composition are also studied, especially in revealing the origin of BC reactivity when it is used as environmental functional materials. Finally, the reactivity expression and its practical value of LBC have been discussed, which provide a certain theoretical basis and scientific support for its future development in resources recovery and environmental remediations.

2. Lignocellulosic biomass conversion for biochar

Generally, lignocellulosic biomass can be converted into biochar via thermochemical treatment. It is mainly composed of carbohydrate polymers (*i.e.*, cellulose and hemicellulose), aromatic polymers (*i.e.*, lignin), extractives (resins, tannins, and fatty acids) and inorganic components (ICs) [52,53]. The fine structure of lignocellulosic biomass is showed detailly in Fig. 1. Cellulose is a kind of polysaccharide molecule, which generally consists of several hundreds to many thousands of β(1–4)-linked glucoses [52]. Hemicellulose is a heterogeneous class of polymers made of different sugar monomers (six and five carbon monosaccharide units), linking the fibers of cellulose into microfibrils and cross-links with lignin, further providing structural strength for plant cells [54]. Finally, lignin (mainly composed of coniferyl alcohol, *p*-coumaryl alcohol, and sinapyl alcohol) is considered as the cellular glue, which provides impermeability, structural support, and standing up to oxidative and/or microbial attack [55,56].

2.1. LBC conversion technologies

LBC can be produced via several sustainable carbonization technologies, which all basically meet the requirements of green chemistry in terms of wastes recycling and efficient utilization [57]. Among these carbonization technologies, slow pyrolysis, microwave carbonization, and hydrothermal carbonization, which mainly retain the solid phase composition, are applied to produce sustainable biochar. While fast pyrolysis, gasification and flash carbonization are commonly utilized for acquiring renewable energy source and process heat, aiming at concentrating biomass energy for bio-oil and bio-gas production, so biochar is generally as a co-product. Fig. S1 have given the brief descriptions of all the LBCTs involved in this section. And the yields of LBC obtained from different LBCTs and operating conditions as well as corresponding technological challenges are shown in Table 2. This section has provided insights into the state-of-art accomplishments in LB conversion and LBCTs.

Pyrolysis. Pyrolysis is the most studied and discussed carbonization technology, and it generally refers to the process that LB raw materials under nitrogen atmosphere and other hypoxia conditions experience a series of thermochemical and physical changes, such as water reduction, removal of volatile substances, generation of aromatic substances and material structure changes [68]. Different morphologic products can be

Table 1
Present situation and application potentials of biochar produced by different biomass sources.

Type	Biomass feedstock	FT (1)	Modification method	SSA (2)	PV (3)	APD (4)	Application potential	Reference
Lignocellulosic biomass-based	Ramie	450	Aging of biochar based on acidizing and oxidation process	42.10	–	4.540	Achieving effective adsorption and removal of cadmium in water	[27]
	Corn straw	500	–	23.50	0.0110	6.000	Realizing the significant reduction of H_2S production in biogas digester without affecting the methane production	[28]
		800	Zinc chloride solution modification	544.00	0.6100	–	Having high electrocatalytic performance, and realizing the effective removal of nitrobenzene in water based on adsorption and electrochemical decomposition	[29]
		900	–	693.09	0.2925	2.294	Effectively activating persulfate and hydrogen peroxide to remove phenolic pollutants in water, and realizing its high mineralization	[30]
	Maple	500	–	161.00	0.0950	3.500	Realizing the significant reduction of H_2S production in biogas digester without affecting the methane production	[28]
	Peanut shell	600	Modification with MgO	–	–	–	Adsorbing phosphate from saline-alkali soil, improving soil nutrients and increasing rice yield	[31]
		700	–	283.00	0.1700	5.260	Having the application potential to catalyze the degradation of antibiotic pollutants in water	[32]
	Pine sawdust	650	–	171.00	0.0750	–	Significantly increasing the number of main active microorganisms in the process of anaerobic digestion, and improving the production of CH_4	[33]
	Walnut shell	500	–	1.64	0.0025	6.165	Reducing the migration rate of cadmium in soil, and having the potential for remediation of heavy metal pollution in soil	[34]
	Rice straw	600	Hydrogen peroxide pretreatment	138.10	–	–	Inhibiting N_2O emission during soil denitrification process, and alleviating greenhouse effect	[35]
	Pomelo peel	300	Potassium ferrate impregnation pretreatment	35.88	0.0244	3.920	Realizing the efficient removal of hexavalent chromium in water through compound adsorption mechanisms such as reduction, electrostatic action and complexation	[36]
	Pomelo peel	900	Hydrothermal carbonization pretreatment at 190 °C for 24 h followed by pyrolysis	1292.00	0.7040	2.179	Possessing remarkable efficiency in removing analgesic and antipyretic drug from water	[37]
	Douglas fir wood	900–1000	–	510.00	0.2100	15.000	As a useful agricultural soil improver, having little effect on the viability of soil bacteria	[38]
	Lodgepole pine	550	–	111.89	–	–	Having the potential to reduce greenhouse gas emissions	[39]
	Litchi peel	850	Hydrothermal carbonization pretreatment at 180 °C for 12 h followed by pyrolysis	1006.00	0.5880	–	An effective and recoverable adsorbent for removing dye pollution from aqueous solution	[40]
	Sawdust of poplar	700	–	572.63	0.2834	1.980	Activating persulfate effectively in a wide range of pH, and continuously repairing the pollution of lipid regulators as well as their metabolites in water.	[41]
		600	–	400.67	0.1825	1.822		
	Pine needle	800	–	146.03	0.0800	2.320	An efficient catalyst for removal of emerging organic pollutants from surface water/groundwater	[42]
Other biomass-based	Pig manure	700	–	32.60	0.0350	4.260	Possessing the ability of adsorption and catalytic hydrolysis of typical pesticides	[43]
		700	Deashing treatment of biochar based on acidification	218.10	0.3150	5.780		
	Sheep manure	500	Deashing treatment of biochar based on acidification	160.53	0.1720	10.030	Having the potential of adsorption and removal of phenothiazine dyes and can be reused many times	[44]
	Rabbit faeces	500	Deashing treatment of biochar based on acidification	21.14	0.0410	8.640		
	Poultry litter	400	–	6.71	0.0350	0.480	Potential agricultural and environmental application adsorbents for the removal of endocrine disruptors in the environment	[45]
	Shrimp shell	800	–	59.00	0.2000	6.700		[46]
		800		594.00	0.9300	3.100		

(continued on next page)

Table 1 (*continued*)

Type	Biomass feedstock	FT [(1)]	Modification method	SSA [(2)]	PV [(3)]	APD [(4)]	Application potential	Reference
		800	Deashing treatment of biochar based on acidification i) Acidification pretreatment of feedstock ii) deashing treatment of biochar produced by pyrolysis	610.00	0.3300	0.900	Having great application potential in the treatment of high salt wastewater and organic wastewater	
	Dewatered sewage sludge	400	–	75.34	–	7.779	An effective strategy of waste controlling with waste, having potential in the treatment of refractory organic pollutants	[47]
		400	–	70.14	0.2240	7.109	Having the potential in simultaneous treatment of landfill leachate and dye pollution	[48]
		400	Modification with nanometer zero-valent iron	59.68	0.2010	6.325		
	Anaerobically digested sludge	600	–	162.70	0.0400	–	Achieving the effective remediation of heavy metal pollution in wastewater system	[49]

(1) FT: formation temperature (°C); (2) SSA: BET-N_2 surface area ($m^2 \cdot g^{-1}$); (3) PV: pore volume ($cm^3 \cdot g^{-1}$); (4) APD: average pore diameter (nm).

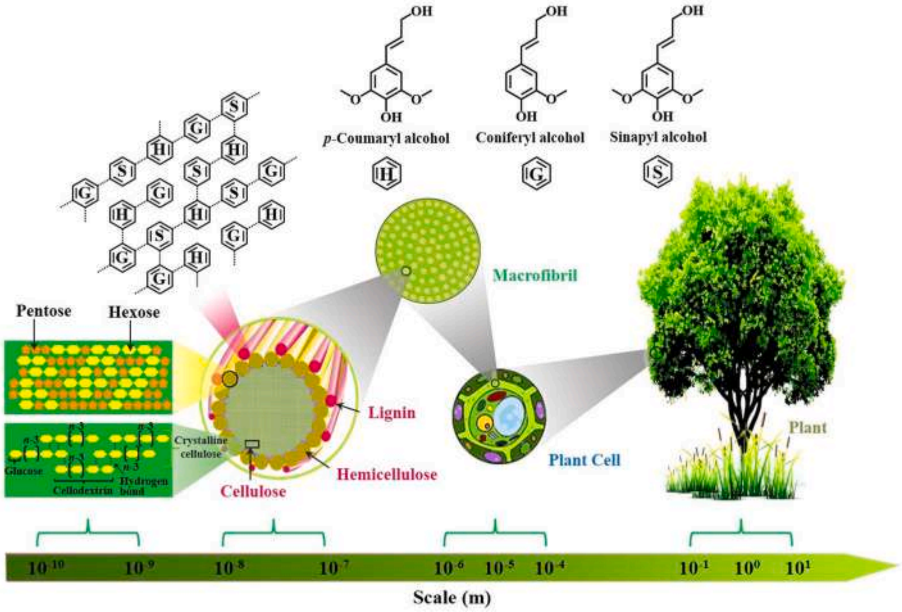

Fig. 1. The main components of LB are cellulose, hemicellulose, and lignin. Microfibrils are made of cellulose, hemicellulose and lignin and organized into macrofibrils for mediation of the structural stability of plant cell wall [52]. Adapted and reprinted from ref. 52. Copyright 2008 the Springer Nature.

Table 2
Solid LBC yields and technological challenges of different sustainable LBCTs.

LBCTs	Typical temperature (°C)	Typical residence time	Typical solid LBC yield (in mass %)	Typical carbon content of LBC (in mass %)	Typical costs	Technological challenges	References
Slow pyrolysis	~700 °C	~Minutes-days	15-89%	≈95%	51-373 US $/tonne biochar	Needing high reaction temperature and controlled heat rates; corrosion of reactor containment	[58–61]
Fast pyrolysis	~300–1000 °C	~2 s	12–27%	≈74%	560 US$/tonne biochar	Rapid removal of solid residues and effective liquids recovery	[60,62]
Microwave carbonization	~200–600 °C	~30 min	25–35%	>60%	650 US$/tonne biochar	The hot spot phenomenon; the need for microwave absorbers	[63,64]
HTC	~180–300 °C	~5 min-12 h	36–72%	<70%	33-87 US $/tonne biochar	Pressure in continuous systems; safety	[19,60,65]
Flash carbonization	~300–600 °C	~30 min	37–50%	≈85%	No information available	Elasticity limit of the materials used for the production equipment	[60,66]
Gasification	~700–900 °C	~10–20 s	5-10%	No information available	380 US$/tonne biochar	Corrosion caused by tars; blockage of particulate filters and clogging of fuel lines/injectors in internal combustion engine	[60,67]

obtained, among which the solid substance is LBC. LBC generation process can be analyzed from two aspects of micro molecules and macro products, and the specific contents are discussed in the follow-up (Section 2.2). Based on the heating environment, heating medium (heat transfer and energy conversion) and heating speed (the rate of temperature rise during manufacturing) [69], pyrolysis can be divided into different types including fast pyrolysis and slow pyrolysis *etc.*, which have been applied in different environments and requirements.

The reaction time and heating methods are the key process parameters. And peak temperature, pressure, particle sizes, vapor residence time, moisture content, inorganic elements, and percent composition of LB components also play important roles in the pyrolysis process [6,70]. Torrefaction (a mild form of pyrolysis at temperatures typically between 200 and 320 °C) [71] or slow pyrolysis has been applied for the production of charcoal through the ages [6]. While fast pyrolysis with high temperature increasing rate and short residence time particularly favors the generation of bio-oil, but inhibits the formation of biochar [7,72]. Recently, many studies focused on increasing the LBC yields for environmental management via adjusting the conditions of preparation [70,73]. Generally, the yield of LBC decreases as the temperature increases until the peak temperature is higher than 700 °C [74]. But increasing the peak temperature, especially above 360 °C, can also result in an increasing content of stable char-like materials further enhancing the stability of LBC in soil [75].

Additionally, the residence time at peak temperature may have little influence on LBC yields because pyrolysis kinetics is mainly governed by the peak temperature [76]. While increasing the pressure of pyrolysis (1.0–3.0 MPa) seems to increase both the fixed carbon (FC) content and the LBC yield (significantly increase the yield of the secondary charcoal and reduce the required energy to sustain this process) [77,78]. Published works also revealed that the yield of LBC was enhanced with the increasing particle size of LB feedstock [79]. This is probably because the diffusion rate of the volatiles through the LBC decreases during pyrolysis, thus the production of additional LBC has been acquired through secondary reactions. Compared to fast pyrolysis, it is not essential to require a fine feedstock particle size (smaller than 1 mm) for slow pyrolysis [6]. Moreover, higher moisture contents (42–62%) of the LB feedstock can increase the LBC yield at elevated pressures [70], while the ICs will also affect the carbonization reaction and the obtained LBC's substance composition, thermodynamic property and reactivity [61].

Microwave carbonization. Microwave production of LBC is a novel LB carbonization technology and it is similar to pyrolysis. The biggest difference between it and traditional pyrolysis is heating mechanism. Microwave is an electromagnetic wave composed of two vertical components, usually known as non-ionizing radiation, which can convert electromagnetic energy into heat energy of microwave heating. Microwave carbonization is usually regarded as a kind of energy conversion process, rather than the traditional heat transfer through medium [80]. The advantage of microwave heating is that there is no requirement for drying and other steps in feedstock pretreatment, because water, as a polar molecule, will play a positive role in the pyrolysis process and be removed eventually. Controllability and energy saving are also advantages, because microwave carbonization technology generates heat faster with less environmental dissipation [81]. On the other hand, the main problems are the requirements of microwave carbonization technology for microwave absorbers in raw materials and the existence of the hot spot phenomenon [82]. At present, the microwave technologies can be divided into catalytic assisted microwave pyrolysis and non-catalytic microwave pyrolysis. And commonly used catalysts include soluble inorganics, metal-oxides, microporous materials and carbonaceous materials [63,83]. On the economic and technical side, the cost per unit of LBC produced by microwave pyrolysis is generally higher than that of conventional pyrolysis. A work by Haeldermans indicates that the lowest selling price of microwave pyrolysis LBC is between €564 and €979 per tonne [84], which can be concluded as a typical cost of about $650 per tonne. But with the decreasing cost of raw biomass and the improvement of microwave equipment, the cost of this type LBC is expected to be reduced.

Hydrothermal carbonization. Hydrothermal carbonization (HTC), also referred to as wet pyrolysis, is a carbonization process of converting LB feedstocks into LBC at 180–300 °C in water for 5 min to 12 h with typical yield of 36–72% (Table 2). Friedrich Bergius first proposed the HTC process in 1913 to describe the process of natural coalification [85]. Most investigations about HTC were related to the production of chemical products as well as the recovery of liquid and gaseous fuels [86,87]. However, recent researches on HTC focused on its solid products (LBC), which have value-added applications in environmental management [18,88]. Furthermore, utilization of HTC technology for biochar from LB feedstocks is becoming increasingly popular for its inherent advantage of using high moisture feedstocks to generate the LBC rich in active functional groups [26,65]. The HTC process occurs in water under self-generated pressures thereby eliminating the cost of drying process, and typically spherical micro-sized LBC with controlled porosity and oxygen-containing groups are generally obtained [89,90]. Its carbonization process are "carbon negative", implying that it is able to reduce emissions from biomass and meet the requirements of carbon sequestration and carbon neutralization [91]. The LBC produced by HTC also can be in turn used in post-functionalization purposes and environmental management due to high reactivity [19]. Notably, temperature is the governing process parameter for the physicochemical properties of LBC produced from HTC. Higher temperature and longer vapor residence time could increase the LBC's carbon content, the extent of energy densification, the amounts of gaseous products, but decrease its yield [65,92]. Moreover, LBC produced via HTC has a relatively lower ash content, higher carbon recovery, and more oxygen-containing functional groups which make it more acidic than that produced via pyrolysis but more readily biodegradable, while LBC from slow pyrolysis is steadier [93,94].

Gasification. Gasification is commonly referred as a thermochemical decomposition of LB with a major objective to produce H_2, CO, CO_2 and CH_4. Technically, in an ideal gasifier, there is no production of LBC because vast majority of LB will be converted into gaseous products and ash. But during the actual operation, a small yield of LBC (5–10%) can be achieved for the partial oxidizing atmosphere and the high operating temperature [70,95]. Therefore, gasification technology is generally used to obtain substances of energy sources and LBC at the same time [96,97]. The specific fractions of the obtained products are depend on the gasification conditions (*e.g.*, activation temperature, residence time and pressure) and the environment (steam or inert gases) prevailing in the process of gasification [70,98]. Moreover, ICs (*e.g.*, Al, Si, Ca, Mg, Fe, P, K, S, Na, Ti and Cl) in LB feedstocks can also be converted to gaseous products [99]. It is a remarkable fact that the LBC produced via gasification may contain higher quantity of alkali and/or alkaline earth metals [100], polycyclic aromatic hydrocarbons (PAHs) [101,102], and dioxins and furans (PCDD/Fs) [103], which are extremely toxic substances generated in high-temperature processes. As a consequence, LBC produced from gasification process may be potentially problematic as soil amendments or water remediation agent [104]. But this kind of LBCTs still possesses several economic and technical merits, such as higher energy density and carbon conversion efficiency of products in per unit LB [96,105]. Additionally, gasification permits continuous LB feedstock feeding and the process heat can be used in LBC-related downstream and/or feedstock-related upstream processes [105].

Flash carbonization. The flash carbonization technology is invented by the University of Hawaii [66,106]. And professor Michael J. Antal and co-workers have taken utilization of flash carbonization to the conversion of LB [72]. Specifically speaking, LB is placed in a vessel with an initial pressure in the range of 1–2 MPa and the flash fire is periodically lighted at the bottom of the LB feedstock where the carbonization time decreases with the increasing pressure. Under this condition, the volatile matters (VMs) in LB are converted into gaseous fuel, and the remaining fixed carbon is derived into LBC [72]. The total flash carbonization process is less than half an hour, and the temperature is conditioned by heating time, water content of the LB feedstock, and the delivered air [66]. Compared with traditional pyrolysis and HTC, the preparation time of LBC is shorter (short-time process with high temperature and pressure), the resulting LBC contains higher microporous components, and its yield is about 40% [107].

Techno-economic analysis. In the cost estimation of LBC production, specific factors such as heating temperature, residence time and yield are the specific factors that affect the cost of LBCTs. Different production process parameters, various biomass size and market conditions all will lead to different production costs of LBC. In Shabangu's paper, the base break-even selling prices of slow-pyrolysis LBC at 300 °C and 450 °C are $220 and $280/tonne, respectively [108]. In another work, the cost of conventional pyrolytic LBC is between €436 and €886 through technical and economic costing [84]. In general, the feedstock price, the equipment construction cost (different methods have different requirements for production environment, equipment and material properties), run manufacturing expenses (such as heating energy consumption, factory scale and production yield) and operating human cost (worker management, transportation and storage, etc.) are main factors that should be taken into account in LBCTs [69]. In Table 2, comprehensive considerations are given to the reported values of literatures and typical costs were provided, hoping to provide reference for the cost accounting of LBC. In addition, the evaluation of cost and price of LBC by full life cycle assessment is also worthy of attention [109], and its potential application in carbon neutralization effectively improves the efficiency of LBC production and LBCTs application.

2.2. Conversion pathways and mechanisms

LBCTs have been discussed, as shown above. Notably, LBC conversion is an extremely complex thermochemical process, including molecular bond breaking and binding, molecular structure isomerization and repolymerization of small molecules generated after cracking, *etc*. This reaction process is generally accompanied by a series of chemical and physical changes, in which chemical changes are mainly the diversified chemical reactions and substance changes generated in the pyrolysis process, while physical changes mainly include the transformation of physical state and energy. Elucidation of LB conversion and LBC formation mechanisms in these processes will be helpful to guide the development of more efficient biochar preparation techniques and achieve the directional preparation of highly active biochar. Therefore, in this section, the transformation mechanism of main components in LB (cellulose, hemicellulose, and lignin) is discussed. And each component is transformed at different degrees and via different pathways and mechanisms.

2.2.1. Cellulose conversion

Compared with hemicellulose and lignin, the structure of cellulose is the most ordered and simplest in LB. The last few years, growing researchers has endeavored to explore the cellulose conversion [110,111]. The process of cellulose conversion is greatly affected by temperature, including primary and secondary conversion [112]. Based on the cellulose pyrolysis reaction model proposed by Kilzer, it is generally believed that there are two competitive reaction paths for the primary pyrolysis transformation of cellulose [113]: i) cellulose is dehydrated to produce cellulose derivatives, CO, CO_2 and H_2O; ii) the other is the depolymerization of cellulose into levoglucosan and tar *etc*. Among them, the dehydration reaction of cellulose will form active cellulose or dehydrated cellulose. Subsequently, cellulose derivatives will be further transformed under excessive reaction temperature or longer residence time, resulting in secondary reactions such as aromatization and

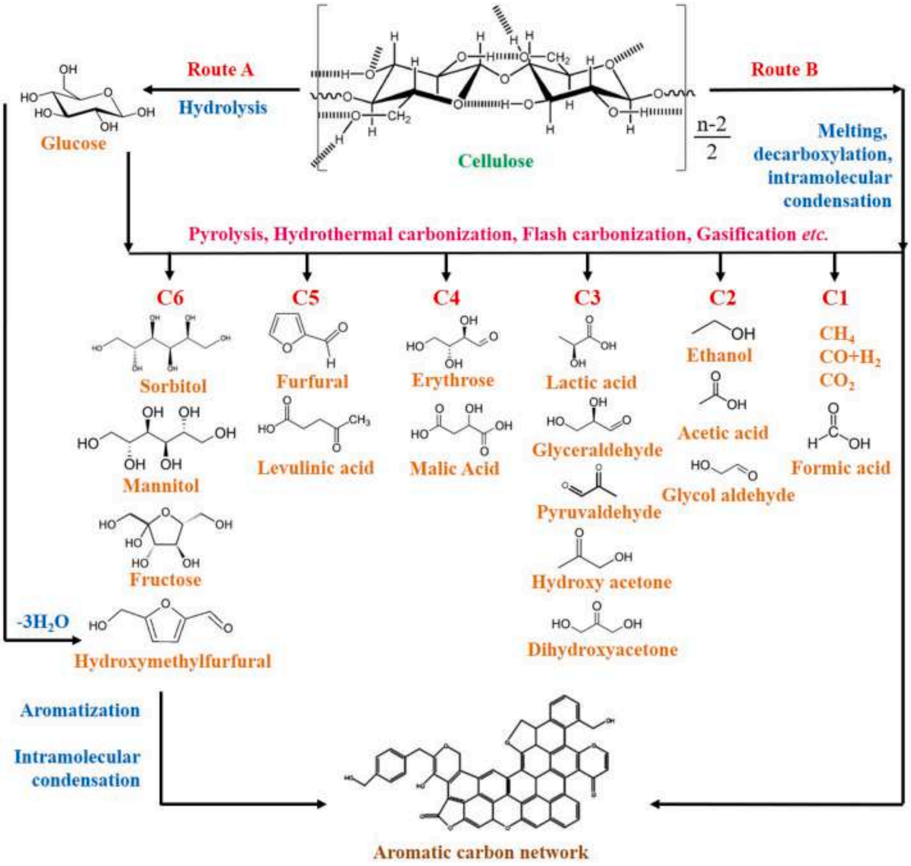

Fig. 2. LBC and potential chemicals from the conversion of cellulose [116,118]. Adapted and reprinted from ref. 116. Copyright 2011 the Royal Society of Chemistry; Adapted and reprinted from ref. 118. Copyright 2011 the Royal Society of Chemistry.

repolymerization of small molecules, further producing LBC [16,113]. Potential chemicals, including LBC, from the conversion of cellulose are presented in Fig. 2. A total of 27 components are identified via GC-MS analysis of cellulose and its surrogate pyrolysis [114,115]. The main products are furfural, levoglucosan, hydroxymethylfurfural, acetic acid, formic acid and aldehyde compounds [7].

Titirici et al. [116] investigated the HTC of microcrystalline cellulose as well as rye straw, and studied differences between cellulose/rye straw derived LBC and biochar derived from D-glucose in morphology and chemical structures. The final LBC structure is switched from a carbonaceous poly-furan rich in oxygen-containing groups to an aromatic carbon network with extended aromatic domains (Fig. 2). Moreover, this LBC also exhibits a well-developed carbon skeleton structure which is formed during the early stage of HTC process. In the process of gasification, LBC is formed via crosslinking reactions, and retains the morphology of the original LB [105]. As temperature increases, LBC becomes progressively higher in carbon and more aromatic due to the removal of carbonyl, hydroxyl, C–H bonds and C=C groups. And volatile matters will be released at the higher gasification temperatures from open spaces in LBC porous structure. Moreover, higher temperatures may cause softening, melting, and mixing of structure. And the shrinkage of the carbon networks could occur at temperatures in excess of 500 °C, accompanied by aromatization reaction [99,117].

2.2.2. Hemicellulose conversion

Hemicellulose is commonly with the chemical formula $(C_5H_8O_4)_m$ and polymerization degree of 50–200. It is an amorphous polymer, usually composed of five different sugar units: D-xylose, L-arabinose, D-galactose, D-glucose and D-mannose. Due to its strongest activity, the conversion reaction can take place quickly at the lower temperature [119]. The transformation mechanism of hemicellulose is extremely similar to cellulose, but because of the five-carbon sugar structure, its main products are often the furan derivatives [7]. Potential chemicals, especially LBC, from the conversion of hemicellulose are shown in Fig. 3. Shanks and colleagues [120] investigated the products from fast pyrolysis of hemicellulose extracted from switch grass. Sixteen products have been identified and quantified (accounting for 85% of the mass balance), and the impacts of inorganic salts (KCl, NaCl, $MgCl_2$ and $CaCl_2$) and switch grass derived ash on the distribution of products were also investigated. Results showed that the ash and inorganic salts increased the formation of LBC and the emission of CO_2. Notably, the conversion process of hemicellulose is considerably different from cellulose, which can be attributed to the cleavage of glycosidic bonds.

In contrast of the cellulose pyrolysis, the temperature corresponding to the hemicellulose decomposition is significantly lower than its branched and amorphous structure [121]. Devolatilization has essentially ceased at temperatures beyond 500 °C, and the further slight mass loss is mainly caused by the releasing of small molecular products in the process of condensation to form LBC. Moreover, the O-acetyl groups in hemicellulose can be cleaved into small molecular radicals, or dissociated, which can stabilize the large molecular radicals and further inhibit the condensation for LBC. And the carbonization mechanism reveals that furfural is an important intermediate in the production of hemicellulose based biochar [122,123]. Notably, due to the higher mineral content of hemicellulose biomass which could promote the autocatalytic carbonization process, the yield of biochar derived from hemicellulose biomass is higher than that from cellulose biomass [124]. And after the demineralization of hemicellulose biomass, the biochar produced by its pyrolysis is also significantly lower than that produced by xylan (a type of hemicellulose).

In the process of hemicellulose conversion for LBC, dehydration and breaking of less stable linkages occur at 150–240 °C for xylan and 150–270 °C for glucomannan; depolymerization occurs at 240–320 °C for xylan and 270–350 °C for glucomannan; charring happens at 320–800 °C for xylan and 350–800 °C for glucomannan [125]. During dehydration and breaking of less stable linkages, methanol is formed via the fragmentation of the methoxy groups in 4-O-methyl-α-D-glucuronic acid, while formic acid is produced for the rupture of the carboxyl in the hexuronic acids. Furfural formed at low temperature reveals that depolymerization reactions are also possible in the process of dehydration and fragmentation, which provides the basis for the production of LBC [126]. When temperature increases, the glycosidic linkages become highly unstable causing a rapid depolymerization and different anhydro-sugars are formed. Moreover, the pyran rings will be transformed into furan rings which are more stable, explaining the formation of furfural, 5-hydroxymethylfurfural, and 5-methylfurfural by depolymerization of glucomannan [127]. While temperature increases further, the residues become much more aromatic and LBC is produced.

2.2.3. Lignin conversion

Lignin has the highest complexity and the strongest thermal stability among the three components of LB, and is the major focus of LBC

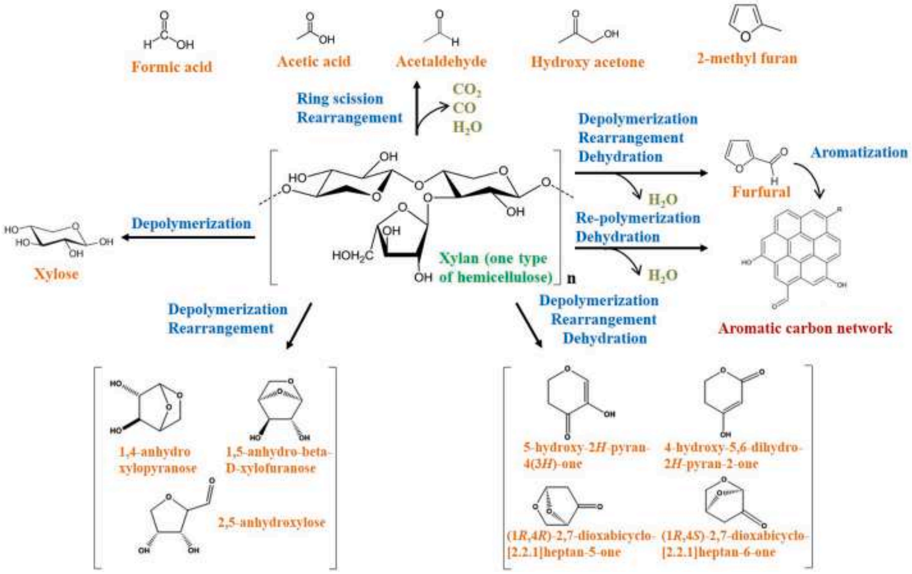

Fig. 3. LBC and potential chemicals from the conversion of hemicellulose [120]. Adapted and reprinted from ref. 120. Copyright 2011 the Royal Society of Chemistry.

conversion research. Lignin is mainly formed via non-phenolic phenylpropanoid units linked with C–C and ether bonds, and its proportions of the monomer units are variable depending on the LB types [56,128]. Its LBC conversion process is also roughly divided into primary transformation and secondary transformation, which is affected by many factors such as reaction temperature, lignin source and pretreatment method [125,129]. The primary conversion process of lignin generally takes place in the low temperature (mainly 200–400 °C), and the guaiacol and eugenol are generated. Through NMR analysis of the products, it is found that C_α-O and C_β-O bonds will be broken during this conversion, while the C–C and CH_3–O bonds demonstrate excellent stability [130]. With the further increase of temperature, the methoxyl structure begins to become active, and lignin will undergo secondary transformation mainly through the homolysis of the O–CH_3 bond, intramolecular rearrangement and alkylation reaction, generating phenolic products such as catechol, triphenols and cresol, and finally producing LBC after molecular repolymerization and aromatization [55].

Early researches on lignin transformation mainly focused on the monomer model compounds of lignin, among which guaiacol and eugenol are the simplest and typical ones. The pyrolysis product of eugenol is mainly coke, while the guaiacol with one more methoxy group is twice as likely to form biochar as eugenol and is the main source of LBC [131]. And with the increase of substituents on the phenol ring, the activity of the intermediates will strengthened significantly, which is helpful to the occurrence of LBC formation [132]. For further studying the conversion mechanism of lignin monomer model, combined with density functional theory (DFT), Huang [133] and Liu [134] calculated various cleavage ways and corresponding bond dissociation energies (BDE) of typical monomer model of lignin as well as the reaction energy barriers of various possible processes (demethylation, demethoxy, free radical rearrangement, *etc.*). And the main processes and calculation results are shown in Fig. 4, Tables 3 and 4. It was found that processes (1) and (2) were the most important path, while path (3) was the competitive reaction path, and the activity of these paths were arranged in the order of (2)>(1)>(6)>(5)>(4) based on the results of energy barriers. Among them, paths (3) and (4) were also the dominated formation mechanisms of LBC precursors (O-methylene benzoquinone) during lignin pyrolysis. Moreover, Huang et al. also detailly studied the potential energy profiles of three main paths (Pathways (1), (2) and (3) in Fig. S2 correspond to the paths of (1), (4) and (2) in Fig. 4b, respectively), and analyzed the specific transformation processes of monomer model compound, which further supported the conclusion of Fig. 4. Similar results of DFT analysis also appeared in the researches of Liu [135] and Wang [136]. The primary pyrolysis mainly occurs in the homolysis or demethoxy process of O–CH_3, while the production of small molecular gas products from the secondary pyrolysis is related to the functional groups in side chain, such as aldehyde group, hydroxyl group and methoxy group. Thus, the pyrolysis mechanisms of monomers in biochar conversion from lignin are mainly O–CH_3 bond homolysis, demethoxy, side face removal and free radical rearrangement reaction.

Table 3
BDE of the major bonds in guaiacol (unit: J·mol^{-1}) [133,134].

Type	Bond	BDE/J·mol^{-1}
D_1	O(8)–C(9)	197.1
D_2	O(7)–H(14)	337.5
D_3	C(2)–O(8)	385.6
D_4	C(9)–H(15)	392.3
D_5	C(1)–O(7)	448.4
D_6	C(3)–H(10)	454.7
D_7	C(4)–H(11)	459.2
D_8	C(5)–H(12)	459.2
D_9	C(6)–H(13)	465.1

With the further understanding of lignin conversion, researchers found that the studies of monomer models cannot reflect the characteristics and effects of lignin polymer. Therefore, the focus of conversion researches from lignin to LBC began to shift from monomer model to dimer model. Through several pyrolysis experiments, more than 8 types of bond have been determined and the β-O-4 bond is the major type of linkage in lignin structure, occupying 46–60% of the total linkages [137]. Phenylethyl phenyl ether (PPE) and its derivatives are the main model compounds, among which PPE is the simplest β-O-4 lignin dimer.

Notably, there is a debate about the pyrolysis mechanisms of β-O-4 bond. In the early days, researchers thought it was dominated by free radical mechanisms. Chu and co-workers [138] studied the transformation of lignin at 250 °C and 550 °C using ethylene oxide-O-4 lignin as the model compound. They identified about 25 volatile compounds via pyroprobe-GC-MS, and proved LBC was probably formed via random repolymerization of radicals. The proposed pyrolysis mechanisms of lignin model compound are shown in Fig. 5. The β-O-4 bond breaks (cleavage 1 in Fig. 5) at temperatures between 250 °C and 350 °C. And the generation of radicals after C_β-O homolysis cleavage is considered to be the starting procedure for the reaction of free radical chain. These radicals can extract protons from weak O–H or C–H bonding (*e.g.*, C_6H_5–OH) to forming products [138,139]. Moreover, H-abstraction, rearrangement, isomerization, double bond formation and concerted reaction will diversify the distribution of products (See reaction (c) and (d) in Fig. 5) [138,140]. LBC is formed via the polymerization of small radical species (such as alkanes, alkenes and aromatics), and this reaction will propagate with more radicals which leads to further polymerization (See reaction (e) and (f) in Fig. 5). And the polyaromatic LBC is eventually generated after the elimination of hydroxyl, methoxyl, and other functional groups [138,141].

With the deepening of cognition, many scholars began to agree that free radical mechanism and synergistic cleavage reaction coexist in the conversion process from lignin to LBC. Huang et al. [142] calculated and

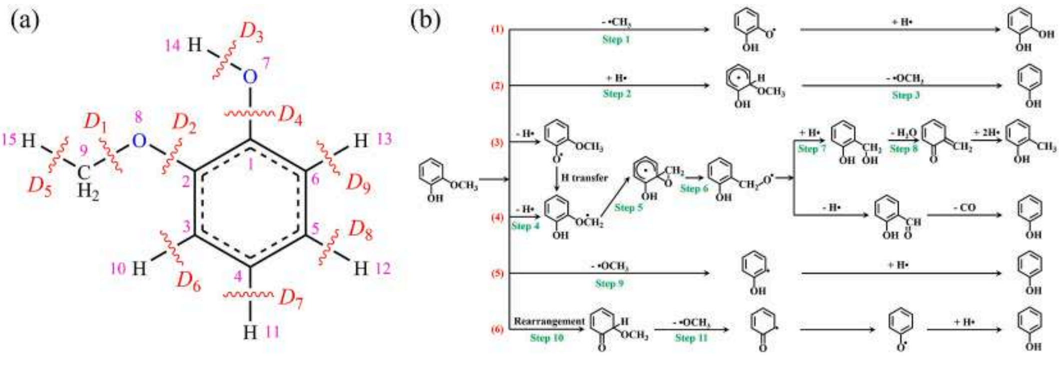

Fig. 4. Various possible transformation processes of typical monomer model of lignin proposed by Huang et al. [133] and Liu et al. [134]. (a) Chemical structural formula of guaiacol and its nine homolytic cleavage ways. (b) Specific transformation pathways of guaiacol. Adapted and reprinted from ref. 133. Copyright 2013 AIP Publishing LLC. Adapted and reprinted from ref. 134. Copyright 2014 Elsevier B.V.

Table 4
Energy barriers of part reaction steps in guaiacol pyrolysis (unit: kcal/mol) [133,134].

	Step 1	Step 2	Step 3	Step 4	Step 5	Step 6	Step 7	Step 8	Step 9	Step 10	Step 11
Energy barrier	47.78	3.70	10.28	94.60	19.13	0.13	31.44	31.98	92.43	82.53	37.37

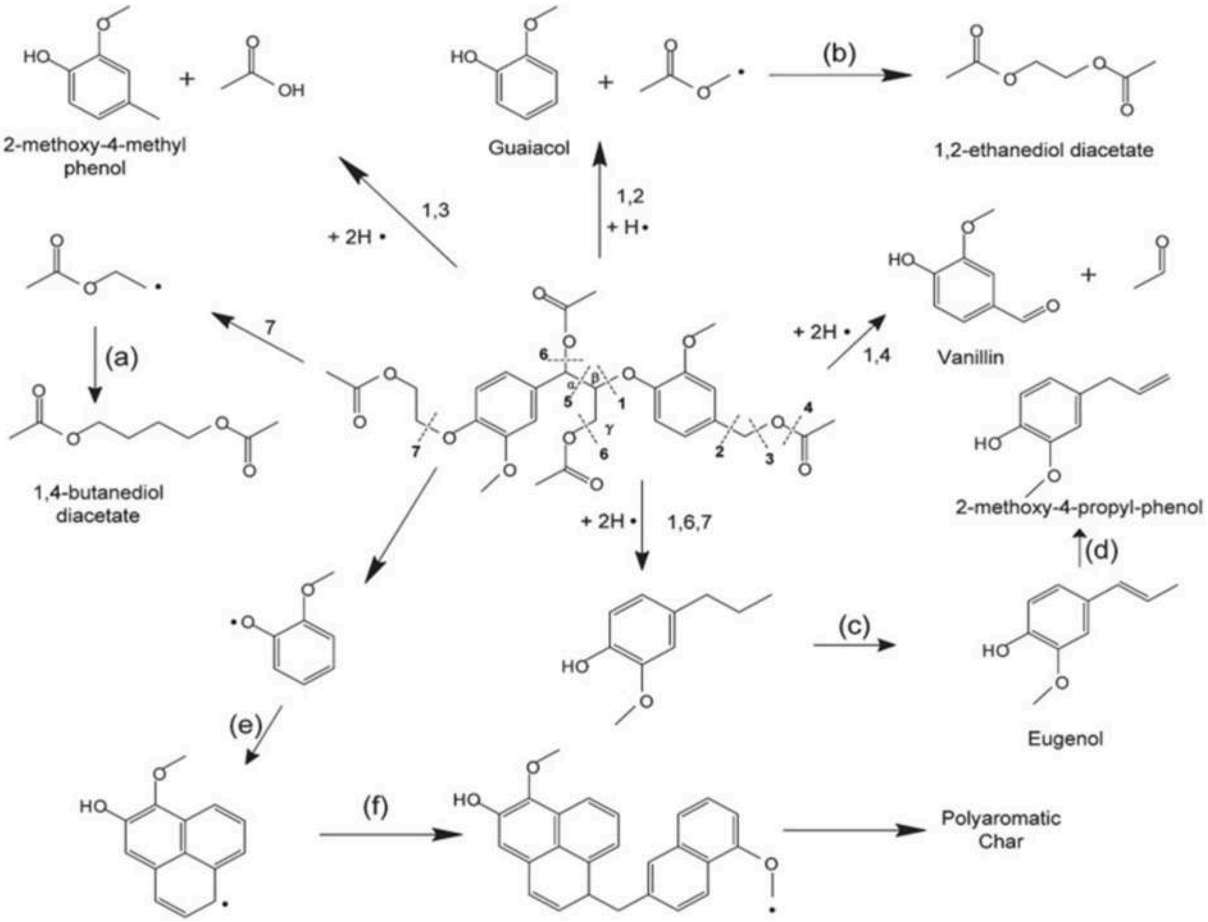

Fig. 5. The proposed pyrolysis mechanism of lignin model compound [138]. Adapted and reprinted from ref. 138. Copyright 2013 John Wiley and Sons.

studied the pyrolysis mechanism of PPE via DFT, comparing the BDE and the activation energy of chemical bond cleavage in the initial pyrolysis process, and pointed out that the two processes exist at the same time. Subsequently, Huang [143] also simulated the carbonization process of β-O-4 lignin dimer model compound (1-phenyl-phenoxyl-1, 3-propanediol) by DFT, and calculated the effect of temperature on the conversion process. Fig. 6, Tables 5 and 6 showed the calculation results of the cleavage ways (mainly C_β-O, C_α-C_β) and the main reaction pathways (homogeneous cracking and synergistic reaction processes) based on the β-O-4 type lignin dimer model compound. It was proved that the synergistic mechanism at low temperature is better than the mechanism of free radical homogenization, while free radical homogenization is dominant at high temperature, which is consistent with the research results of Elder and Beste [144]. They also proposed that the energy barrier of synergistic reaction is slightly lower than that of homogeneous cracking, and the synergistic reaction is mainly carried out according to the mechanism of reverse olefin decomposition. To sum up, the existing studies showed that the transformation mechanism from β-O-4 lignin dimer model to LBC is mainly Maccoll elimination reaction, reverse olefin decomposition reaction, C_β-O homolysis reaction and C_α-C_β cleavage reaction. However, due to the limitation of computing resources and time as well as the complexity of the system, researchers have done little researches on the trimer model compounds of lignin. Meanwhile, the deep transformation mechanism between dimer model and trimer model is still incomplete and needs to be further studied.

Notably, when LBCTs are applied to practical LB, the LBC conversion process will become quite complex. And lignin will be slightly altered by low-moderate temperature pyrolysis. Thus, the conversion of practical LB into carbonaceous materials with the same morphology and properties as that from D-glucose model still requires deep-going research [145,146]. In order to maximize energy densification and LB utilization, a new method containing different temperature regimes is necessary. Moreover, novel and efficient catalysts should be developed to facilitate the effective reaction pathway through hydrolysis-dehydration and elude the strong resistance against hydrolysis, especially taking up-scaling application of LBC production into consideration [147].

2.2.4. LBC formation

As described above, the up-to-date knowledge about the conversion from LB to LBC including carbonization technologies, cellulose conversion, hemicellulose conversion and lignin conversion has been reviewed. Previous studies [118,148] generally accepted LBC as an undesired by-product in the process of LB pyrolysis for bio-oils, syngas and process heat. However, the by-product is trendy to become black gold for its extensive new applications [19,149]. This section reviewed the LBC formation mechanisms comprehensively.

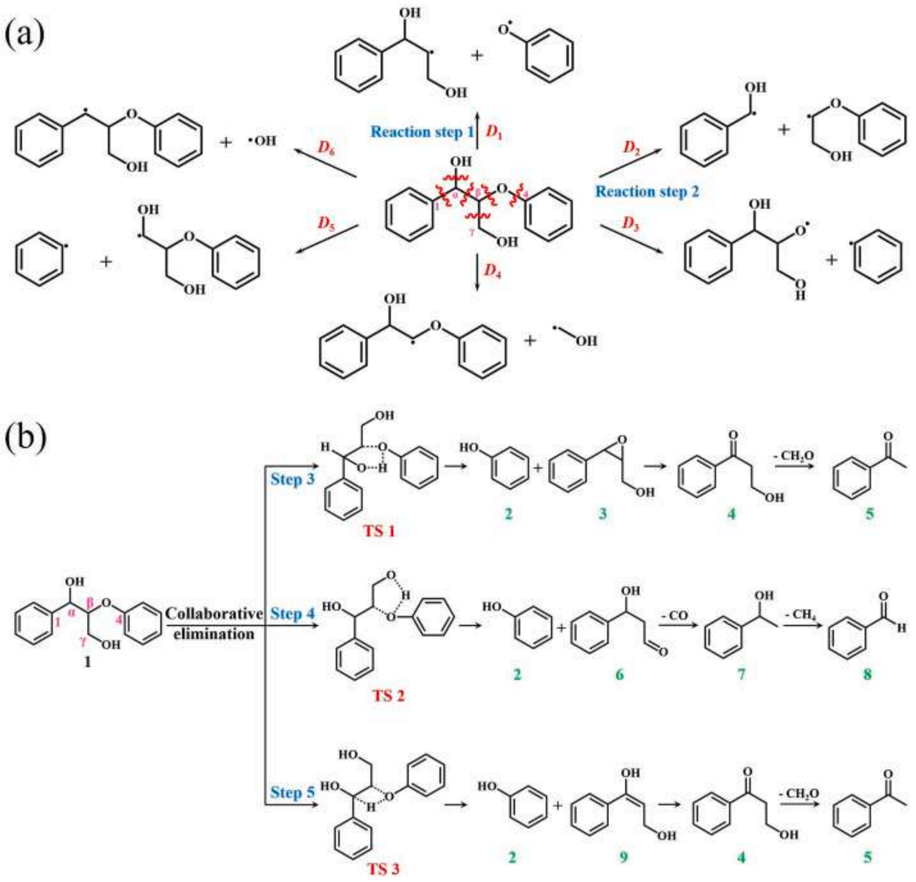

Fig. 6. The homogeneous cleavage ways and the main transformation pathways based on the β-O-4 type lignin dimer model compound, proposed by Huang et al. [143]. (a) Six ways of homogeneous cleavage. (b) Three possible synergistic reaction pathways in transformation processes of model compound. Adapted and reprinted from ref. 143. Copyright 2014 Elsevier B.V.

Table 5
BDE of β-O-4 type lignin dimer model compound in Fig. 6(a) (D_1 and D_2 are the main paths).

Type	D_1	D_2	D_3	D_4	D_5	D_6
Bond	C_β-O	C_α-C_β	O–C_4	C_β-C_γ	C_1-C_α	C_α-O
BDE/J·mol-1	245.3	259.2	380.5	323.9	374.4	303.5

Table 6
Activation energies of initial reaction steps in Fig. 6 at different temperatures.

T (K)	Activation energies (kJ/mol)				
	Step 1	Step 2	Step 3	Step 4	Step 5
298	245.3	259.2	257.1	240.1	219.3
450	244.2	258.9	256.9	239.9	220.1
600	242.4	257.6	256.6	239.6	220.5
750	240.1	255.6	256.2	239.3	220.7
900	237.5	253.1	255.7	239.1	220.8
1100	233.7	249.3	254.8	238.9	220.6
1300	229.5	245.1	253.8	238.5	220.1
1600	223.0	238.4	252.3	237.8	219.0
1900	216.2	231.4	250.5	236.8	218.0

Reaction step 1: D_1, step 2: D_2, step 3: 1→TS 1, step 4: 1→TS 2, step 5: 1→TS 3.

The typical formation mechanisms of LBC (including polymerization of condensed phase species, gas-phase repolymerization, dehydration of biopolymers and repolymerization) have been proposed. The dehydration of biopolymers (without depolymerization) is the main mechanism at relatively lower temperature in the process of slow pyrolysis, while in fast pyrolysis, LBC is usually difficult to maintain the original structures, indicating that repolymerization is the dominant mechanism for LBC formation [114,150]. It is noteworthy that the process of LBC formation can be described as an autocatalytic process because the inorganic components, especially the alkali metals and alkaline earth metals (such as K, Ca, Mg), are able to catalyze the LB pyrolysis [151]. In this part, the formation of LBC (including coke and char) from slow and fast, thermal and catalytic pyrolysis of LB feedstock and corresponding model compounds are comprehensively concluded. Generally, char is the residue generated by thermal deconstruction, while coke is defined as the catalytic product. In this review, the solid residues formed in LB pyrolysis, slow or fast, thermal or catalytic is named as LBC. The formation of LBC is mainly caused by dehydration, polymerization, decarboxylation, and decarbonylation of furanic compounds, anhydrosugars, fragmented oxygenates and/or olefins. Fig. 7 illustrates the representative mechanisms involved in LBC formation.

The pathway of toluene self-alkylation (RA in Fig. 7) is via alkylation (RA.1), dehydrogenative coupling (RA.2), isomerization (RA.3), hydrogen transfer and repetition (RA.4). The coke formation pathway is via alkylation on the methylbenzene with carbenium ions (RB.1), side alkylation and isomerization (RB.2), cyclization (RB.3), as well as repetition of RB.2, RB.3 and RB.4. The formation of char from furfural is via Diels-Alder cycloaddition (D-A cycloaddition) with propylene and isomerization (RC.1) as well as aldol condensations (RC.2~RC.7). The pathway RD includes D-A self- or hetero-cycloaddition (RD.1) of C-6 and C-5 anhydro-sugars, D-A cycloaddition of RD.1 products with the original anhydro-sugars (RD.2), and repetition of RD.2, followed by the enol-keto tautomerization to generate carbonyl ending groups and the condensation combining polyaromatic rings terminated by hydroxyl and carbonyl groups (RD.3) [152,153]. Moreover, the minimum projection

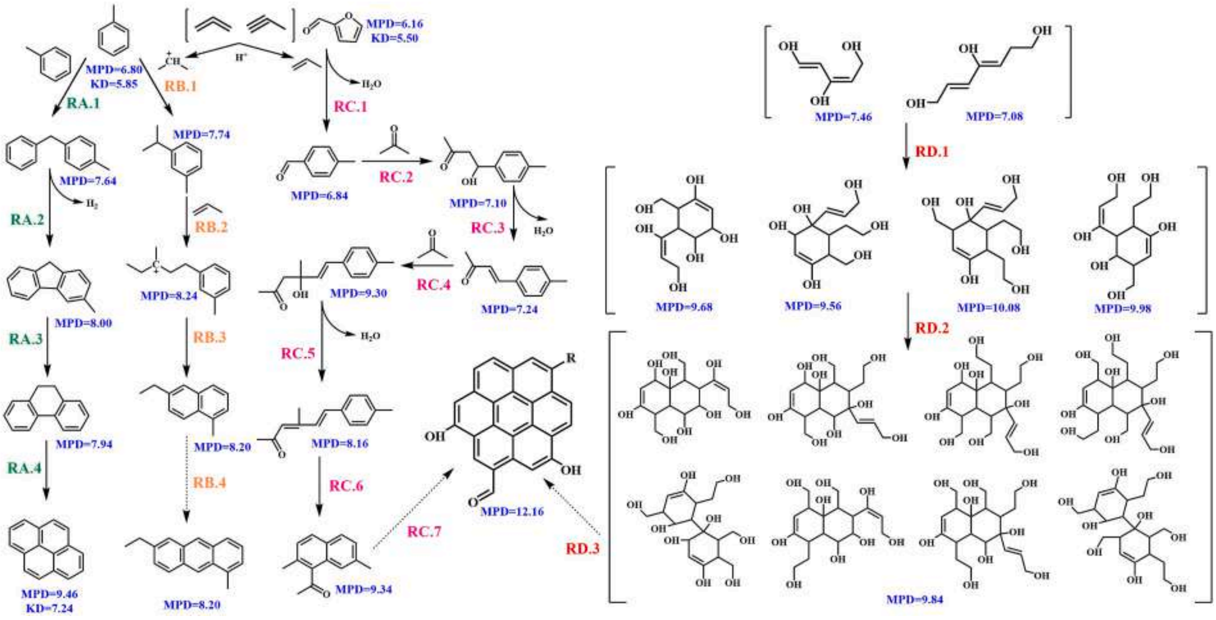

Fig. 7. Possible reaction pathways for the formation of LBC (char and coke) [152]. Adapted and reprinted from ref. 152. Copyright 2013 the Royal Society of Chemistry.

diameter (MPD) of each molecule and their kinetic diameter (KD) are also presented in Fig. 7 [154]. Notably, these reaction mechanisms are not exhaustive, which can only be considered as representations. LBC produced from practical LB is much more complex than that from model compounds of LB and much works still remains to be settled by researchers to elucidate the specific LBC formation mechanisms.

3. Characterization of LBC

The structure and composition of LBC have determined its properties. The commonly used LBC characterization techniques and their corresponding characterization structures and compositions are listed in Fig. 8.

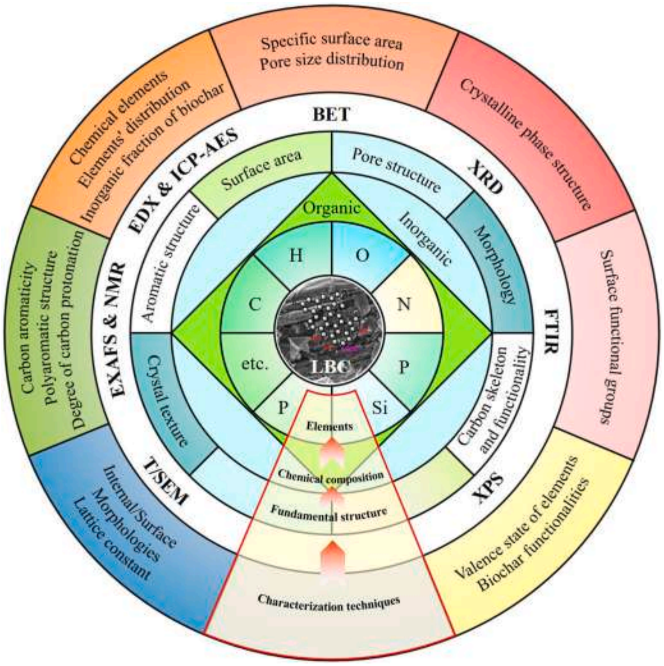

Fig. 8. Physicochemical properties and common characterization techniques of LBC.

3.1. Fundamental structure of LBC

The basic structure of LBC mainly includes specific surface area (SSA), pore structure, morphology, aromatic ring structure (ARS), crystal texture and carbon skeleton structure (CSS). SSA, pore volume, and pore size are highly contingent on the kind of LB and the LBCTs conditions. LB usually possesses 0.1–3.2 m^2/g surface area contributed by the nature mass transmission channel pores [155]. In the pyrolysis process, SSA and pore volume of LBC generally increase significantly, and its degree is improved with temperature [61]. This may be due to the gradual gasification of simple molecules formed by the cracking of VMs such as ethylene and esters from outer surfaces of LB [156]. In addition, the pore structure and SSA of LBC are significantly affected by its inherent mineral composition [157]. Notably, one significant change in LBC structure compared to the original LB is that the surface is more uneven and coarse, which is resulted by the non-smoothness microspheres generated from carbon recombination or fiber decomposition in LB decarboxylation reaction [90]. The size of these microsphere particles is generally in the range of 1–3 μm. And the pore structure of LBC is mainly composed of medium and large pores at low treatment temperature, while is mainly composed of quasi-fine nanopores and micropores at high treatment temperature [51,156].

ARS, CSS and crystal texture are also very important basic structures of LBC. The formation of carbon rings and their condensation into larger structures dominated by flake and stack are always considered as the fundamental sources of ARS, while the interwoven links of carbon nets constitute the CSS of LBC [158]. The content of ARS in LBC affects its fate and reactivity in the environment, while the CSS and CT reveal the heterogeneous structure of LBC and also play a decisive role in its function in environment [159]. To investigate these structures in LBC, solid ^{13}C NMR, Raman spectroscopy, EXAFS and XRD were applied [160].

LBC is principally amorphous with some local crystalline structure. Dynamic molecular structures of two kinds of LBC (wood and grass) under pyrolysis temperature from 100 to 700 °C was reported by Keiluweit [58]. The results are shown in Fig. S3. Four distinct categories of char (LBC) have been proposed: (i) the crystalline structure of the LB can be preserved in transition chars; (ii) the incipient aromatic polycondensates and heat-altered molecules are randomly mixed in amorphous chars; (iii) composite chars are composed of poorly ordered graphene stacks, which are embedded in amorphous phases; and (iv) turbostratic chars are mainly disordered graphitic crystallites. These molecular structure variations affect the durability of LBC in soil and/or water and function as sorbents and/or catalysts. XRD test results also showed that LBC had a large content of amorphous phase in the carbon matrix structure, accompanied by a small number of high conjugated lamellar aromatic structure or stacking structure cross-linked with random crystal structure [58,161]. And with the increase of pyrolysis temperature, the grain size of LBC increases, and the overall structure of carbon frame tends to be more ordered [58,162].

The scientific understanding of the skeletal structure in LBC has gone through the process from hypothesis, structural calculation and actual observation. Based on the ideal development of LBC structure, Lehmann [163] studied the evolution process of CSS in LB carbonization: with the increase of treatment temperature, the CSS was transitioned in the order of amorphous aromatic carbon, conjugated aromatic carbon and graphitized carbon. Subsequently, Brewer and co-workers [164] characterized the structure of LBC from fast pyrolysis and gasification by quantitative calculation of ^{13}C NMR, and proposed an aromatic clustering model of LBC based on its aromatic structure characteristics. Cao et al. [165] also measured the changes in the aromatic clustering structure of LBC at treatment temperature from 300 °C to 700 °C by NMR, and the results to some extent supported the rationality of the aromatic clustering model. Recently, Professor Chen [166] simplified the calculation of the CSS model of various LBC by taking H/C atom ratio as the parameter based on the rectangular polycyclic aromatic model, and calculated the clusters of molten aromatic structure in LBC at different pyrolysis temperatures. In addition, many researchers have used NEXAFS to study the aromatic structure of LBC, such as its aromaticity and degree of aromatic condensation [58,167]. Heymann [168] tried to estimate the aromaticity of LBC through the spectral deconvolution of functional group distribution by NEXAFS spectroscopy, and verified its polyaromatic structure according to the mechanism of multiple scattering resonance.

It is worth noting that the basic structures of LBC cannot exist independently. The change in one structure type often leads to the change in other types of structure [51,169]. For example, the development of pore structure and SSA is mainly contributed by the ARS components of LBC, thus the variation trend of SSA and porosity with LB treatment temperature is similar to that of aromaticity [156]. Therefore, it is necessary to link the relationships among the various structures, and to improve the understanding of the basic structures in LBC by considering more different calculations and observations from both partial and holistic perspectives. In addition, due to the limitations of previous studies and the difficulty in fine structure studies, the researches on the fine skeleton model and crystal structure of LBC at various conversion conditions remains to be further explored.

3.2. *Reactivity related composition of LBC*

The composition of LBC is an important index to determine its function, reactivity and application. Therefore, this section mainly focuses on the chemical composition and element composition related to reactivity of LBC as well as the changes of corresponding components in LBC conversion process, aiming at laying foundations for the later discussion about the function and surface reactivity of LBC.

Macroscopic perspective. The composition of LBC can be roughly divided into organic components (OCs) and inorganic components (ICs). Among them, OCs mainly include the FC and VMs of LBC, while ICs mainly refer to ash part (*i.e.*, the mineral components of LBC) [170]. Table S1 presents the chemical composition and related properties of some typical LBC.

As the principal part of LBC, FC is the basis of its structure and the carrier of functionality, and generally refers to the organic solid part after the VMs are driven off [171]. Since FC and VMs have significant influence on the stability and reactivity of LBC, some applications of LBC, such as carrier, adsorbent and catalyst, all have certain requirements on their contents [172,173]. Generally, the production of LBC is mainly aimed at obtaining the FC part of its OCs and ensuring the appropriate contents of other active organic components, so as to realize the controllable regulation to different functionalities of LBC. But the process of LBC is a physicochemical process which is difficult to control structures and has incomplete transformation [174]. Therefore, the OCs of LBC obtained through a variety of methods have a wide range of variations [26]. For instance, the increasing of treatment temperature and the prolonging of treatment time will significantly increase the tendency of VMs in LBC transforming into gaseous and liquid products, and make it easier to be separated from the LBC system with processing atmosphere [175]. Additionally, the decrease of VMs is the direct cause of the increase of FC content, which is consistent with the rule of data in Table S1.

The ICs in LBC are minerals in the form of ash inclusions. These minerals play an important role in the carbonization process of LB, which not only influences the formation of LBC infrastructure, but also is an important component of LBC reactivity bringing self-catalysis functionality [169]. Mineral compounds (MCs) in LBC ash mainly include potassium salt, SiO_2, silicate, carbonate, phosphate and the oxides/hydroxides of mineral elements such as Ca, Mg, Al, Mn, Zn, or Fe [163,176]. And these MCs generally exist in two states in LBC: i) mineral phase (*i.e.*, pure mineral salt form), and ii) composite state combined with surface functional groups in LBC (*i.e.*, containing chemical bonds in forms of metal-C bond and metal-O-C bond, *etc*. [177]. MCs in the form of pure mineral salts is generally the source of direct catalytic ability of reactivity, while the bonded form of MCs plays the role of electron transfer as a special structure. Table S2 has summarized the composition and content of the common mineral elements in different LBC, mainly including P, K, Ca, Na, Mg, Al, and Fe *etc*. In addition to the mineral constituents included in Table S2, LBC derived from grass, rice husk and nut shells *etc*. would significantly contain more amorphous silica than other LBC (>2%) [178].

Notably, except the accumulation of ash, the increase of pyrolysis temperature may also lead to the transformation of the structure and crystal form of MCs in LBC, making them more crystallized and less soluble [179,180]. Sun and colleagues [181] reported that, when the pyrolysis temperature increased to 900 °C, Fe in ash of coconut shell biochar would undergo a phase transition from $FeCl_2/FeCl_3/Fe(NO_3)_3$ to α-Fe/Fe_3C, and its solubility also gradually decreased. A similar phase conversion process could also occur in other typical MCs (such as Ni, Mg and Si) of LBC during the heat treatment of LB [178,179,182]. And possible reactions which could occur in the inorganic phases mainly include dehydration, dichlorination/denitration/decarboxylation and

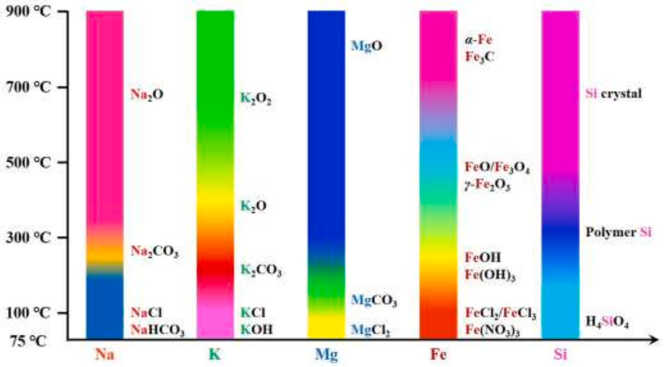

Fig. 9. Possible chemical transformation of mineral elements during the pyrolysis process from LB to LBC (the gradual change of color represents the gradual change of substance composition). Cited from the corresponding references: Mg [182], Si [180], Fe [179,184].

reduction *etc.* [183]. Fig. 9 summarizes the possible phase transition paths and laws of several typical MCs during pyrolysis process from LB to LBC (Mg [182], Si [180], Fe [179,184]). Based on the phase transformation rules of these mineral elements in LB carbonization, researchers explored and developed various functional LBC materials by using the reactivity properties brought by its mineral composition [185,186]. It is not difficult to see from above that the ash components (*i.e.*, the MCs) of LBC is indeed an important source of LBC functionality.

In summary, the OCs of LBC lay the foundation of its structures (including carbon frame structure and aromatic structure, *etc.*), while the interaction between ICs and OCs further improves the structures and plays role as the component of active sites providing functionality and reactivity for LBC. However, the carbon stability of OCs, the fine structure of ICs (such as the types of some mineral elements, crystal types and mixed crystal structures), and the specific interaction mechanism between OCs and ICs are still unclear and not systematic, which need further study and discussion.

Microscopic perspective. Element is the cornerstone of substance structure and function. The carbonization of LB is actually a process in which various elements undergo physical and chemical transformation to produce different species [169]. The elements that compose LBC mainly include C, H, O, N and some mineral elements (shown in Tables S1 and S2). These elements have different contents in LBC, and their combination with each other constitutes its different structures and reactivity units [187].

i) *Carbon, hydrogen and oxygen.* They are the most dominating elements in LBC [188]. And their existing forms in LBC can mainly be divided into: i) inorganic phase, existing in mineral salts such as carbonate and bicarbonate, ii) organic phase, combined to form the lipid ring structure and ARS, organic compounds in VMs, and active functional groups (AFGs) components on LBC surface [169,188]. Among them, C is the most basic and important element, and its content is generally the highest among all elements. In requirements of some processes, the main purpose of LBC production is to obtain highly enriched C components from LB including persistent free radicals (PFRs) centered on carbon [174]. As for H, although its content is small (generally accounting for 1%–6% of the total mass of LBC), it constitutes important active components in LBC such as hydrogen bonded and AFGs [189]. And its composition and structure are often needed to be indirectly characterized by analyzing and measuring other elements [160,169]. Regarding the O element, it is involved in the formation of nearly all functional groups on LBC surface, including hydroxyl group, epoxy, carboxyl, acyl, carbonyl, ether, ester and sulfonic group, and plays important roles in the chemical reaction behaviors of LBC [169,188].

The composition of C, H and O or the ratios of H/C and O/C are often used as the evaluation indicators for the particular characteristics and structures of LBC, such as aromaticity and functionality [190,191]. Manyà and co-workers [78] reported that there was an obviously negative correlation between H/C and O/C ratios and the aromaticity of LBC. And Spokas [192] found that the smaller the O/C ratio was, the more stable the LBC was and the less it aged. Besides, C, H and O, whether in organic or inorganic (mainly organic) phases, will undergo significant changes in composition and morphology under the influence of temperature. In the inorganic phase, when the pyrolysis temperature gradually increases, these three elements will break away from LBC system due to the crystal transformation of mineral salts [184,193]. While in the organic phase, the increasing temperature promotes the cleavage, decomposition and aromatization reactions of organic structures in LBC, leading to the loss of large amounts of small molecules (such as CO_2, H_2O and H_2). Additionally, since C, H and O in the organic phase occupy the majority of total C, H and O elements, their composition or changes of H/C and O/C ratios can generally reflect the structure changes in the whole LBC [167,194].

ii) *Nitrogen.* N is the most abundant element in LBC except for C, H and O, which is mainly existing in peptide bonds and proteins formed in LB during plant growth and development [195], and generally absorbed by plants from the growing water/soil environment in the form of NO_3^- or NH_4^+ [196]. Due to the different absorption and utilization of N in various growth stages and different parts of plants, the N content of LBC derived from corresponding LB is generally different [195,197]. For example, leaves (such as grass leaves and bamboo leaves) are the parts needing large amounts of N to synthesize in the process of plant growth and development, so the N content of LBC produced from them is higher than that derived from tree trunks (with low content of chlorophyll and protein) [188,198]. Moreover, the N species in LBC generally presents in the organic part with the forms of protein peptide bond, amine, imine, amide, nitro, nitroso, pyrrole and pyridine, while the inorganic part mainly exists in forms of NO_2^-, NO_3^- and NH_4^+ [199]. And during the pyrolysis process, with the increase of temperature, the N in organic part of LBC will be transformed from the protein-N and amine-N in the original LB into heterocyclic N such as pyrrole and pyridine accompanied with the aromatization of the C element [156,200]. When the temperature rises to a very high level, the graphitic-N may be also formed [200].

Additionally, similar to O/C and H/C ratios, C/N ratio is also an indicator of the properties of LBC, which reflects the effectiveness of LBC as a soil nutrient and is generally little affected by temperature [200,201]. And because LBC contains a certain amount of N, itself could be regarded as an N-doped material, which has wide applications in fields of environment and energy storage [135,202,203]. Furthermore, based on the transformation processes and rules of N species in LBC, scientists have applied the nitrogen-doped modification methods in material synthesis to modify the electronic band structure of materials and use it as the active sites of various reactions [204,205]. At present, the development of novel N-doped carbonaceous materials has become a hot topic in the field of environment.

iii) *Other elements.* In addition to the four main elements mentioned above, there are P, Si and trace metallic mineral elements in LBC. In most cases, the content of P and Si depends on the type of LB, while the mineral elements make up only a small part of LBC [198,206,207].

P is another essential nutrient element in plant body (LB precursor), which is generally absorbed by plants from surrounding environment in forms of $H_2PO_4^-$ and HPO_4^{2-} [208]. Most wetland plants can effectively enrich P, so the LBC derived from them tends to have higher P content [188]. Some studies have confirmed that element P mainly exists in organic form (such as nucleic acid, phospholipid and adenosine phosphate) in LB, while exists in ash with forms of pyrophosphate, phosphate and other inorganic substances in LBC [209,210]. This is probably due to the thermal instability of organophosphorus in plants. Even in the low-temperature pyrolysis process, it is easy to produce inorganic phosphorus compounds through dehydration, condensation and decomposition [211,212]. Unlike N, P compounds (below 700 °C) are extremely difficult to volatilize, thus P in LB will eventually enter into LBC phase even after a series of thermochemical reactions, exhibiting certain intrinsic reactivity in the form of ash [188,213]. Therefore, with the increase of pyrolysis temperature, the total P content of LBC generally shows an overall rising trend. Notably, if P is transferred into the non-LBC phase, the P content in LBC would change inversely with temperature [214].

Compared with P, the existence of Si is more selective in LBC. Only Si-loving plants (such as rice, corn, wheat, and barley) using Si as a nutrient possess a lot of Si in their bodies [206,207,215]. And presence of Si is mainly related to plant adverse resistance (pest resistance, drought resistance and toxic heavy metals resistance, *etc.*) [216,217].

Whether in LB or pyrolytic LBC, Si principally exists in inorganic forms [218,219]: i) silicic acid and easily soluble polymerized Si in LB, ii) crystalline Si in LBC. Xiao and colleagues [180] confirmed this by the conversion experiment of Si in straw LBC at different pyrolysis temperatures, and pointed out that Si would dehydrate and polymerize to form crystalline Si along with the carbonization of LB. Moreover, Si basically constitutes the main part of ash in LBC converted from Si-rich LB, and its formed silicic acid after entering solution system shows significant promotion effect of LBC for removing heavy metals and other substances [187,220]. Notably, In the Si-rich LBC, C and Si have the mutual protective effect during the pyrolysis process, which prevent the loss of each other at different temperature stages [180].

As for metallic mineral elements closely related to reactivity of LBC, in previous discussions, the composition, structure and pyrolysis transformation rules of them have been analyzed in detail, which are not repeated here. It is worth mentioning that alkali and alkaline-earth metals (A&AEMs) are important components of fast-growing plants and mesophyll cells, so LBC derived from this kind of LB is more likely to retain more A&AEMs (such as timothy grass presented in Table S2) [221]. While heavy metals (HMs) are mainly found in LBC converted from plants with high enrichment capacity of HMs (*i.e.*, hyperaccumulators) [222,223]. During the LBC conversion process, almost all the HMs are retained in the LBC phase, and few of them ($<2\%$) will flow into the non-LBC phase [224]. In addition, due to the special atomic structures, HMs may interact with carbon matrix structures of LBC to form PFRs (such as semiquinones, cyclopentadienyls, and phenoxyls) thus providing LBC with strong reactivity [225]. Fang and co-workers demonstrated this point detailly in their research [226]. It could be seen that mineral elements significantly affect the structures and functions of LBC, so it is of great value and significance to carry out further researches and explorations.

4. The reactivity of LBC

The reason why the reactivity of LBC has received a lot of attention in chemical or biological reactions because it endows LBC with many active centers as the interface of the reaction, including AFGs and free radicals, which have strengthened its electron transfer ability and inherent reaction function. Also, there are studies showing that hydrogen bonds, interface effects and nanometer pores on LBC surfaces can enhance its adsorption properties and improve the efficiency of chemical reactions indirectly [51]. The discussion on the origin of these active sites is an important basis for studies of pollutant removal principles and sustainable remediation strategies. Therefore, this section has focused on reactivity of LBC (mainly AFGs and PFRs) and traced its origin during the process of LBC conversion.

4.1. Surface functionality mediated reactivity

The functional groups in LBC are typically located at the binding sites of the O and heteroatoms (mainly N and S) on the surface of the carbon rings. Based on this, surface functional groups can be roughly divided into nitrogen-containing (NFGs), sulfur-containing (SFGs) and oxygen-containing functional groups (OFGs) [227]. Notably, the OFGs are intrinsically generated in general, while heteroatoms such as S and N may be bound to the surface of LBC in quantity through surface modification like doping, sulfonation or nitrification [228,229]. Similarly, LBC surface functional groups can be also divided into aliphatic and aromatic groups, and the functional groups that have been mainly concerned and discussed are carboxyl, carbonyl, hydroxyl and ester groups because of their higher abundance and activity [187]. As for PFRs, they are generally formed in LBC surface during LB pyrolysis in the presence of transition metals (TMs), remaining active for a long time in the environment [230]. A large number of experimental studies and evidences show that AFGs and PFRs constitute the main body of LBC functionality, and play important roles in promoting LBC-mediated reaction [20,231,232]. Table 7 summarizes the typical surface functionality mediated reactivity and its abundance as well as functioning mechanism in the actual reaction.

Oxygen-containing functional groups. Among the OFGs on LBC surface, carbonyl groups (C═O) have been regarded as one of the most important groups. Derivatives derived from the C═O bond, including aldehyde, ketone and quinone groups, have been found to contribute significantly to the enhancement of the electron accepting capacities (EACs) of LBC [246] and the catalytic reactivity towards oxidants [247]. In the work of Zhang and his team [248], the contribution of surface functional groups of barley grass LBC to EACs was explored. They carried out multiple linear regression between the functional group contribution and EACs, and found that the quinone groups were the main sites improving electron acceptability, especially under the high temperature condition. Moreover, study of Wu and co-workers also pointed out that the electron exchange capacity of LBC materials was positively correlated with the existence of C═O bond functional groups, and both quinone and hydroquinone structures contributed greatly in promoting electron exchange [249]. As mentioned above, the carbonyl groups on the surface have significantly enhanced the electron-mediated ability of LBC. So, during the catalytic activation of persulfate or H_2O_2, the production of hydroxyl radical or sulfate radical can be easily facilitated via LBC. This point have been verified in the researches of both Wang [250] and Duan [251]. Additionally, there are also studies claiming that quinone groups contribute to the formation of singlet oxygen [252,253], so the formation and regulation, abundance and distribution of carbonyl groups on the surface of LBC deserve further explorations.

Besides carbonyl groups, among the OFGs on LBC surface, carboxyl groups and hydroxyl groups are also worthy of attention, which not only affect the hydrophilic/hydrophobic properties and surface charged properties of LBC, but also contribute to the degradation of pollutants in the LBC-contamination system [254]. Uchimiya et al. [255] adopted cottonseed shell as feedstock of LBC, and then used it for the stabilization and removal of HMs after the oxidation of sulfuric acid and nitric acid. It was found that the oxidized LBC was rich in carboxyl groups and showed higher removal capacity to lead, zinc and copper. In the study of Chen, the removal rate of ammonium by LBC after hydrochloric acid treatment was significantly improved, which was also attributed to the increase in the abundance of carboxyl groups and hydroxyl groups on surface [256]. Notably, the carboxyl groups and hydroxyl groups are also conducive to electron transfer of LBC, which has been proved in the work of Li and his co-worker [257].

Heteroatoms-containing functional groups. The studies of functional groups containing heteroatoms on the surface of LBC mainly focuses on N and S atoms. The NFGs mainly exist in forms of $–NH_2$, -NH- and –C═N-, while the SFGs refer to C–S, C═S, or S═O structures [258,259]. In general, among NFGs, quaternary-N and pyridinic-N are more stable [260]. The literatures have claimed that NFGs have a prominent performance in catalytic redox reaction [261], and nitrogen-doped LBC owns a higher capacitance and stability when used as a capacitor [262]. This is due to the fact that the introduction of N atoms have enhanced the production of positively charged C atoms, which will accelerate the interaction between substances and surface structures of LBC, characterized by the enhancement of LBC reactivity [240]. At present, the most extensive studies about NFGs in LBC still exist in the adsorption and catalytic removal of environmental pollutants, especially HMs and organic pollutants [263–265]. SFGs also perform well in removing pollutants from water (as listed in Table 7). In addition to the traditional means like sulfonation, Zhang [266] transplanted SFGs in the skeleton structure of LBC via means of plasma. And the removal rate towards pollutants of modified wheat LBC has greatly increased from 26.4% to 95.5%. Notably, if the introduced S is mixed into carbon rings instead of forming the active functional group structure, it may destroy the charge balance of the covalent carbon electron system and disrupt the charge redistribution [240], which will have a negative effect on reactivity of

Table 7
A summary table of typical surface functionality mediated reactivity.

Type of dominated surface functionality	LBC preparation method	Abundance (or concentration) of surface functionality	Activated oxidant	Functionality mediated reactivity	Generated active species	Reference
Oxygen-containing functional groups	Hydrothermal and pyrolysis of Wood chip	Carbonyl groups (14.39%)	PDS	High amount of C=O group in LBC could transfer electrons to PDS to generate $SO_4^{\cdot -}$	$SO_4^{\cdot -}$, $\cdot OH$	[233]
	A modified sol-gel method, slow pyrolysis of bamboo powder	Oxygen-containing functional groups (such as –OH and –COOH groups) (38.08%)	PDS	Oxygen functionality could be served as active sites transporting electrons for PS to generate radicals	$\cdot O_2^-$, $SO_4^{\cdot -}$, $\cdot OH$	[234]
	Carbonization of Peanut shells at 300–900 °C	-COOH groups, ketonic C=O groups (NA [(a)])	PDS	-COOH and ketonic C=O of LBC were the essential electron donors for PDS activation to induce the formation of free radicals	$\cdot OH$, $\cdot O_2^-$, $^1O_2$	[235]
	Pyrolysis of Coconut shell at 700 °C	C=O groups (NA)	PMS	Electron-rich oxygen functional groups on LBC acted as electron mediators enhancing PMS activation	$SO_4^{\cdot -}$, $\cdot OH$, $^1O_2$	[236]
Nitrogen-containing functional groups	Pyrolysis of corncob biomass and urea at 700 °C	Pyridinic N (6.56%) Pyrrolic N (2.61%)	PDS	Edge nitrogens (pyridinic N and pyrrolic N) facilitated the interaction between LBC and PDS to form surface-bonding complexes	Surface-bounding reactive complexes	[237]
	Pyrolysis of Boehmeria nivea biomass fiber and urea at 900 °C	Graphitic N (47.84%) Pyridinic N (32.54%)	PMS	The positive charge on the adjacent carbon of graphite nitrogen induced the PMS molecules to lose electrons to produce $^1O_2$ through nucleophilic reactions	$^1O_2$	[238]
	One-step calcination of sawdust and nitrogen-containing organic compounds as raw materials	Graphitic N (48.28%) Pyridinic N (37.68%)	PMS	The nitrogen-rich LBC could more easily transfer electrons to the O–O bonds in PMS and activate PMS to produce reactive radicals	$SO_4^{\cdot -}$, $\cdot OH$, $^1O_2$	[239]
	Pyrolysis of reed biomass and ammonium nitrate at 900 °C	Graphitic N (61.66%)	PDS	PDS molecules were strongly bonded with active N sites to form metastable surface-confined reactive species	Surface-confined activated persulfate-carbon complexes	[203]
	Impregnation-pyrolysis process of rice straw with Urea	Graphitic N (NA)	PMS	Graphitic N could enhance the positive charge of the neighboring C atoms, and thus boosting their interactions with negatively charged HSO_5^-	$SO_4^{\cdot -}$, $\cdot OH$, $^1O_2$	[240]
Sulfur-containing functional groups	One-step pyrolysis of wood shavings and thiourea	Thiophenic S (NA)	PMS	Sulfur moieties altered their surrounding electron density, making it favorable for PMS activation	$SO_4^{\cdot -}$, $\cdot OH$, $^1O_2$	[241]
	One-step pyrolysis of nanocellulose and thiourea	-C-S-C- groups (NA)	PMS	Electron-rich -C-S-C- groups could enhance the asymmetric spin-charge density of adjacent carbon atoms, facilitating the breaking of O–O bonds	$SO_4^{\cdot -}$, $\cdot OH$, $^1O_2$	[242]
Persistent free radicals	Pyrolysis of bamboo at 500 °C	Semiquinone radicals (7.94×10^{18} spins·g^{-1})	H_2O_2	Electrons were easily transferred from PFRs to H_2O_2, achieving activation of H_2O_2	$\cdot OH$	[243]
	Pyrolysis of corn stalk at 500 °C	Semiquinone radicals (9.67×10^{18} spins·g^{-1})	H_2O_2	Electrons were easily transferred from PFRs to H_2O_2, achieving activation of H_2O_2	$\cdot OH$	[243]
	Wet impregnation method with one-step pyrolysis	Persistent free radicals ($\sim 2.3 \times 10^6$ a. u.)	H_2O_2	PFRs on the surface of LBC could directly activate H_2O_2 to generate $\cdot OH$	$\cdot OH$, $\cdot O_2^-$	[244]
	Pyrolysis of hyperaccumulator biomass containing Mn and Zn	Persistent free radicals ($8–10 \times 10^3$ a. u.)	PDS	Electrons were easily transferred from PFRs to PDS, achieving activation of PDS	$SO_4^{\cdot -}$, $\cdot OH$, $^1O_2$, $\cdot O_2^-$	[245]

(a) NA: not available.

LBC to a certain extent and need to be avoided. Although some present studies (such as researches in Table 7) have been carried out on the surface functional groups containing heteroatoms on LBC represented as S and N, the research on the technology of heteroatomic functional groups and the influence of manufacturing conditions is still lacking. It is necessary for scientists to further explore how to avoid the negative effects of heteroatomic functional groups, increase their content quantitatively and controllably, and strengthen contributions of reactivity given to LBC by them.

Persistent free radicals. Another functionality of concern is the PFRs, which are formed via the decomposition reaction of organic components in LB (like catechols) and the electron exchange between them and TMs during the pyrolysis process [267]. Conceptually, PFRs can remain reactivity in the atmospheric environment for hours or days and mainly include structures like cyclopentadienyl, phenoxyl and semiquinone [268]. And mediating the process of electron transfer is the main mechanism of its function in LBC [243]. In current studies on PFRs of LBC, the most commonly utilized characterization method is electron paramagnetic resonance (EPR), and the spectral factor of EPR, g-factor, can represent the types and concentrations of PFRs. Further, PFRs are usually divided into carbon-center and oxygen-center free radicals based on g-factor. The former is less than 2.0030, while the latter is greater than 2.0040, and g-factor between the two values are considered to be the PFRs containing adjacent oxygen atoms [269,270]. The presence and the function of PFRs on LBC surface was not clear in earlier studies. Through using an analogy between LBC and activated carbon, the researchers found that one possible explanation for the oxidizing ability strengthening of H_2O_2 via LBC is the reception and conduction effects of electrons by PFRs. With the development of researches, the contributions of PFRs on LBC to the activation of H_2O_2, persulfate and O_2 have been proposed [271–273]. In the study of Fang and his team [226], the combination of salicylic acid trapping techniques and EPR have been adopted to investigate the performance of LBC in catalytic activation of H_2O_2, and found that the generation of ·OH was correlated positively with the consumption of PFRs. Moreover, studies on the activation of persulfate [231] and degradation of pollutants like p-nitrophenol [232] by PFRs on the surface of LBC have also demonstrated its functionality and reactivity. Some similar studies are listed in Table 7. However, the long-term activity maintenance of PFRs is also a double-edged sword. There is studies demonstrating that PFRs on the surface of LBC have a negative effect on the plants' germination and growth, such as maize, wheat and rice seed, which should not be ignored [230,274].

4.2. *The origin of LBC surface reactivity*

Due to its good performance in promoting reaction or removing pollutant, LBC attracts wide attention, and research on the origin of LBC reactivity has also become necessary. The various active sites (especially AFGs and free radicals) of LBC mentioned in the previous section are exactly the embodiment of reactivity, and the conversion process of generating these active sites in the original LB have revealed the origin of reactivity. During the preparation of LBC, the most profound factors affecting LBC's inherent functionality and reactivity are heating temperature, continuous heating time and LB feedstocks [275]. In addition, the reactivity of LBC can be also improved by means of preoxidation, loading or doping [160]. Therefore, in this part, the origin of LBC reactivity will be introduced from two viewpoints: the inherent effects of LBC conversion process (endogenous transformation) and modification methods (exogenous strengthening).

Endogenous transformation. The conversion process of LBC is the continuous decomposition reaction of macromolecular organics in LB and the separation/formation reaction of functional groups. And the changes about chemical properties related to the origin of LBC surface activity mainly include atomic ratio, element composition, structural change and generation of active species. Most active functional groups all will undergo a process from generation trend to functionality enrichment in the process of endogenous transformation. In detail, at the beginning of pyrolysis, the sensitive free hydroxyl groups will react with carbon ring structures in LB before the evaporation of water to form OFGs, followed by the cracking of interchain hydrogen bonds, and the aliphatic hydrocarbons present a tendency to convert to aromatic hydrocarbons [276]. When the carbonization deepens, with the transfer of electrons, electron-deficient C═O bonds and aromatic C═C bonds will be formed to further enrich surface functionality in LBC after the formation of electron-rich hydroxyl structure [187]. As for PFRs, during the pyrolysis process in which LB and TMs coexist, the quinone or phenolic groups formed in LBC transfer electrons to the TMs and stabilize the charge distribution of molecular structure via the empty electron orbitals in transition metal atoms, and finally resulting in the formation of metastable PFRs on the LBC surface [243]. Fig. 10 shows the transformation process of PFRs from LB to LBC as well as its reactivity for activating AOPs. Generally, PFRs will experience a transition from oxygen-centered to primarily carbon-centered with increasing temperature [268,277]. Therefore, the regulation and control of temperature and residence time in the conversion process are important factors for LBC reactivity.

The existence of S, N and other heteroatoms inherent in natural LB is different in various parts and growth stages of plants, and the content is generally not high (far less than the content of O), which is consistent with what was mentioned earlier. And the sites containing heteroatoms (N and S), after LB pyrolysis at high temperature, will mainly exist in forms of sulfate and nitrate. Therefore, active components containing S or N, existing in LBC, are relatively few through endogenous transformation [188]. However, they still play important roles in regulating the reactivity of LBC [243]. By deeply analyzing and summarizing the transformation of N species in 3.2, Fig. 11 proposes the possible migration and transformation paths of nitrogenous active species during the conversion process from LB to LBC in order to reveal the reactivity origin of NFGs.

Exogenous strengthening. Besides active LBC obtained from

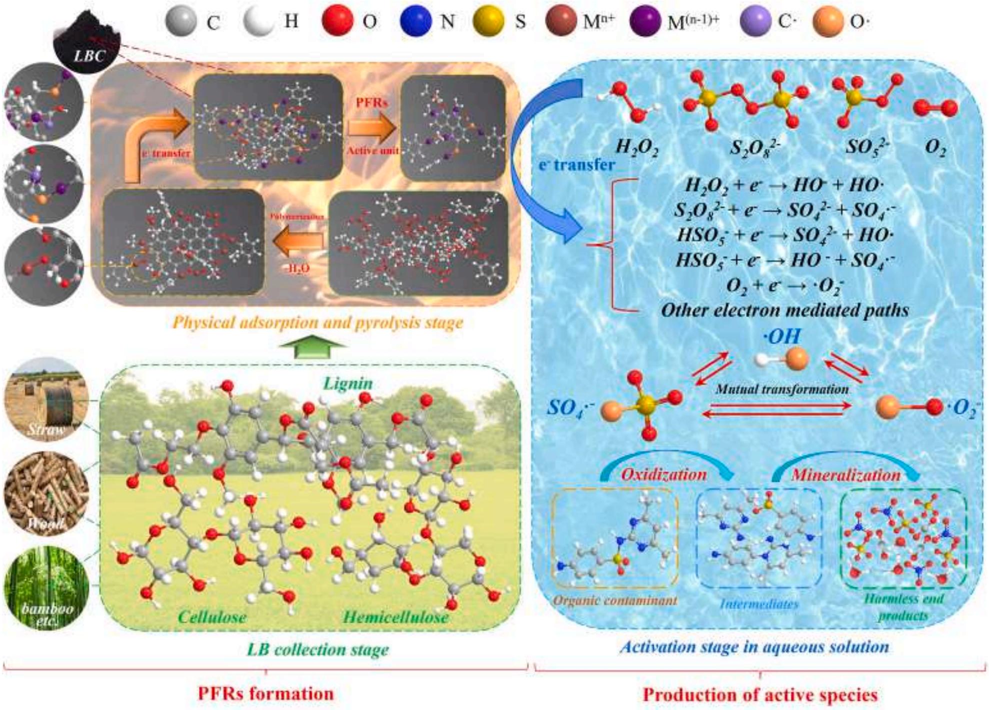

Fig. 10. The formation mechanism of PFRs in LBC and its AOPs (advanced oxidation processes) activation mechanism was proposed [226,231]. Adapted and reprinted from ref. 226. Copyright 2014 the American Chemical Society; Adapted and reprinted from ref. 231. Copyright 2015 the American Chemical Society.

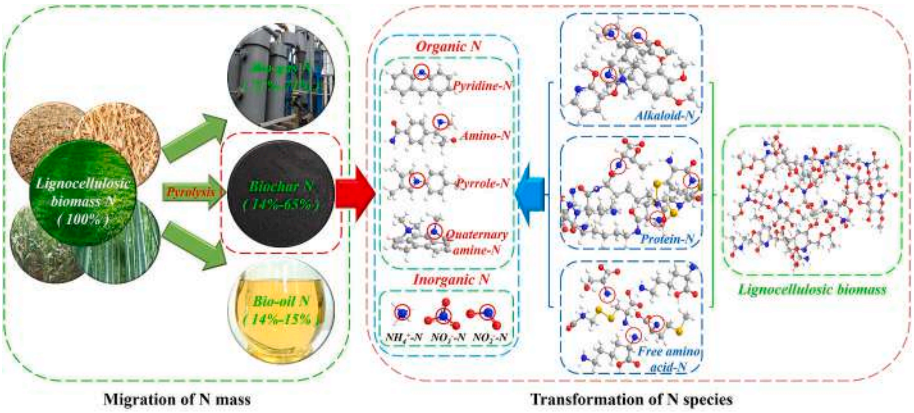

Fig. 11. Migration and transformation of nitrogenous active species during conversion process from LB to LBC.

endogenous substances of LB such as proteins and TMs, functional groups containing O, N or S as well as PFRs can be also largely introduced by means of modification and doping. The main principle is to artificially increase the content of active substance precursors or conditioning agents in the transformation system of LB, and strengthen the endogenous transformation process of precursors, thus significantly improving the conversion rate of reactivity-related components in LBC [23]. The introduction of SFGs is mainly through the reaction with simple S-containing substances, such as hydrogen sulfide, sodium sulfide, potassium sulfide and thiourea, while NFGs mainly depend on the addition of organic substances, such as urea or amine, as well as inorganic ammonium (the process of transformation is similar to that mentioned earlier) [278,279]. As the important modification reagents, the use of acids/bases also play important roles in the formation of carboxylic and hydroxyl groups on LBC surface. Wang et al. [280] treated wheat straw LBC with separate hydrochloric acid and ferric chloride, or a mixture of the two, and found that the removal of contaminants was obviously increased in LBC system after acid modification, which is contributed to the greatly increasing content of carboxyl and hydroxyl groups. Compared with novel plasma methods and other treatments, it is more commonly discussed to load metal oxides or other metal components in LBC. Reactivity from these types of LBC mainly comes from two aspects: i) abundant free active metal components in the produced LBC; ii) the PFRs generated through the bonding between metal and LBC matrix, with greater abundance of PFRs and stronger reactivity than LBC derived from simple LB (transformation pathway is basically similar to that in Fig. 11) [281]. As mentioned above, there are many existing methods to regulate the types and contents of active components on LBC surface for the improvement of its reactivity. However, the discussion on the origin of LBC reactivity needs to be further studied in terms of groups transition, contribution ratio of different components and efficiency of treatment methods.

5. Expression of LBC reactivity

In this part, based on LBC reactivity, the pathways for action of the reactivity are discussed from the perspective of promoting electron transfer, mediating some specific reactions and facilitating the generation of redox active species. This section looks forward to summarizing the reactivity functioning pathways of sustainable LBC and prospecting the future researches from a new perspective.

5.1. *Facilitating electron transfer*

The gain and loss of electrons between different substances are widely existed in the spontaneous or artificial reactions, which have contributed to the complexity and diversity of matter. In earlier studies, direct electron transfer was mostly through conductive iron minerals [282]. As research progressed, biomaterials like conductive carbon materials [283–285] have attracted researchers' attention. Recently, the researches on LBC as electrode material are also increasing gradually [286,287]. Gu and colleagues [288] reported an electrode material made from bamboo LBC, aiming at forming micropores in LBC surface to enhance its electronic conductivity and electro-catalytic property through activation of KOH/annealing process. Despite the fact that the composition of LBC material contains few traditional conductive substances [90], the abundance of functional groups on its surface still makes it become an attractive choice to manufacture electrode materials for capacitors, in which phenolic groups can function as electron-donor while quinone groups and condensed aromatic groups play the role as electron-accepter [289]. LBC derived from the low sulfonated alkali lignin has been adopted by Hu [290] to make a supercapacitor for storing energy, and Jillian L. Goldfarb and co-workers activated the pistachio shell LBC through an alkaline impregnation method and applied it in electrochemical cells [291]. The former reached 96% capacitance retention rates after 5000 charge-discharge cycles with the maximum specific capacitance of 344 F/g and an energy density of 8.1 Wh/kg, while the latter still provided 100% coulombic efficiency after 4000 cycles. Studies have also indicated that the surface functional groups contributed to the overall electron flux of LBC to some extent, but the higher conversion temperature leads to the lower charge and discharge capacity [292]. Therefore, more researches are needed on the influence of preparation method, temperature and LB feedstock in the manufacturing process on the electrical conductivity of LBC.

Another filed deserving concerns is the role of LBC in facilitating electron transfer associated with microorganisms in the environment. Previous studies have shown that LBC can promote electron transfer between microorganisms and substances in soil remediation, enhanced pollutant removal, and wastewater treatment reactors [293,294]. Chen and colleagues [295] investigated the direct electron transfer in the co-culture of several bacteria in the case of ethanol as electron donor. Result showed that bacteria were attached by LBC rather than direct contact to carbon source, suggesting that LBC is the main body to promote electron transfer of carbon source. Yu et al. [246] explored the performance of different rice straw LBC in the degradation of pentachlorophenol by sulfur-reducing bacteria. It was found that the electron transfer capacity brought by surface reactivity of LBC contributed significantly to the degradation process of pentachlorophenol. Wang and co-workers [296] set up two up-flow anaerobic sludge blanket reactors to explore the role of LBC in improving reactor efficiency and promoting electron transfer. After LBC was added, the electrical conductivity of granular sludge increased to 23.29 ± 0.99 μS/cm, which was twice as high as before. Overall, the electrical conductivity is important embodiment of LBC reactivity, and it is contributed to strengthening the processes based on electroactivity through facilitating electron transfer whether between substances or between environmental microorganisms.

5.2. Mediating specific reactions

In the aspect of facilitating chemical reactions, metals and their oxides, including precious metals, are more common catalysts because of its efficiency and sensitivity [297]. However, as the demand for environmental quality rising, catalysts required economic efficiency and environmental friendliness. Due to its high porosity, large surface area and various types of functional groups, LBC has been regarded as an excellent choice during green chemical progress.

Among the chemical reactions mediated by LBC, researches and applications have mainly focused on esterification, hydrolysis, hydration and some nucleophilic reactions like alkali-catalyzed dehydrogenation of compounds [298–300]. J. Mahammad Rafi [301] made LBC from seed shells pyrolysis, and then applied it successfully in promoting the esterification of glycerol and acetic acid, proving that LBC was an effective and reusable catalyst. In general, when LBC is used to improve the esterification efficiency, it should be pretreated, such as sulfonated. Arif Hidayat and co-workers [302] applied the sulfonated coconut shell LBC to the esterification reaction between palm fatty acid distillate and methanol, and studied the reaction kinetics, finding significant improvement in catalytic efficiency. In addition, the effects of different sulfonation methods of LBC on the production of fatty acid methyl esters has been studied by Akinfalabi [303]. LBC's role in the hydrolysis reaction is inseparable from the formation of active sites on the surface, such as $–NH_2$, –COOH and –OH. Rick Ormsby [304] used pine chip LBC for catalyzing the acidic hydrolysis of hemicellulose, while in the study of Xiong and co-workers [305], –COOH and –OH groups of wood waste-derived LBC acted as the active sites in the hydrolysis of maltose. As for the promotion towards hydration by LBC, Liang [306] reported that the lignin-based LBC performed well in the hydration of 2, 3-dimethyl-2-butene. Regarding the nucleophilic reactions mediated by LBC materials, some studies have shown that these reactions are generally performed through functional carbon nanotube structures in LBC [51, 307]. However, due to the complexity of nucleophile reactions, it is difficult to determine the role and influence of LBC. But published studies still suggested that LBC has great potentials and prospects in mediating reaction processes and more studies are needed.

5.3. Generating active species

The presence of abundant AFGs and free radicals on the surface of LBC makes it a good choice to promote the formation of active species in the reaction system, either by itself or in combination with other substances like metals/metal oxides [308]. Many AFGs exist on the surface of LBC like aliphatic and aromatic groups, and carboxyl, hydroxyl as well as ester functional groups get the main attention [309]. Generally, the types and abundance of AFGs are higher on the surface of LBC produced by HTC, while the PFRs on the pyrolytic LBC also appeal to researchers. This section focuses on the most significant expression pathway of LBC reactivity, that is, promoting the production of active species, such as reactive oxygen species (ROS) and $SO_4^{\cdot -}$.

ROS, especially $\cdot OH$, $\cdot O_2^-$ and $^1O_2$, have been concerned and applied because of the active chemical properties in the degradation of organic pollutants [270,310]. Fang and his team [311] reported that the PFRs and quinone-like structures on the surface of wheat straw LBC dominantly contributed to the generation of singlet oxygen and hydroxyl radicals, which could be used in diethyl phthalate degradation. Yang [312] also demonstrated that LBC had excellent performance in transforming O_2 into H_2O_2, and produced H_2O_2 can be consumed through AFGs in LBC to further generate ROS thus to effectively degrade environmental pollutants. Moreover, promoting the production of active species is also the important reflection that LBC plays an important role in Fenton or Fenton-like processes. Rice hull LBC and coconut shell LBC were used by Rubeena and his colleagues [313] to synthesize reactive Fenton catalyst for removing acid red 1 dye, while Fang [231] proposed that LBC could activate persulfate to produce sulfate radical through Fenton-like reactions, thus effectively degrading persistent organic pollutants in environment. There are many similar examples [42,314]. In addition, during the interaction between ozone and LBC, even superoxide radicals can be generated [315–317]. Fig. 12 has summarized the possible pathways for LBC to promote the production of active species based on its reactivity. The above statements all have indicated the great potential of LBC in promoting the production of active species.

Undoubtedly, as novelty way of waste utilization, the application of LBC is beneficial to the sustainable development of human society. However, Liao [230] reported that the use of LBC in the environment may have negative impacts on plant growth and seed germination. Therefore, before LBC is put into large-scale applications, the impact of LBC on soil texture, water condition and atmospheric environment should be also fully evaluated, not only for positive effects brought by reactivity expression, but also for potential negative effects. In addition, it is also necessary to take economic and technical analysis as well as comparison with other treatment measures into consideration, in order to make benign and efficient utilization of LBC reactivity.

6. Conclusion and outlook

The process of fossil resources regeneration relying on nature is slow, so it is a necessary obligation for human beings to make efforts for its sustainable utilization. As a renewable carbon resource, the LB can produce green chemical products during its pyrolysis process, contributing significantly to energy recovery and environmental remediation. This work has reviewed the latest developments in LBC reactivity researches. The advantages and technical challenges of various LBCTs were first summarized from the viewpoint of sustainability. The thermochemical properties of main components in LB (cellulose, hemicellulose and lignin), and the relationship between their carbonization behavior and the distribution of functional substances were discussed. The polysaccharides and side chain structures of cellulose and hemicellulose as well as the basic unit structure and ether bond of lignin significantly affect the LBC conversion behavior of LB (including reaction kinetics of primary and secondary conversion, evolution of aromatization and repolymerization, chemical bond homolysis and free radical process, *etc.*). Emphasis was placed on the formation mechanism of LBC (*e.g.*, polymerization of condensed phase species, gas-phase repolymerization, dehydration of biopolymers and repolymerization), in which the ICs in LB are the self-catalysts of these processes. The relationship between structures and reactivity of LBC was discussed in detail, finding that C, O, N and mineral elements were the important components of its reactivity. C and MCs participate in the formation of PFRs through promoting electron transfer, O is the basic element of almost all AFGs in LBC, while N contributes to the active N species in the process from LB to LBC. More importantly, the exploration of the origin of LBC reactivity provided valuable information for the effective utilization of its active species in surface. And the expression pathways of LBC reactivity were reviewed from the aspects of promoting electron transport, mediating specific reactions and promoting the formation of redox active species. As a comprehensive study, it is expected to provide reference and basis for carbon neutralization strategies and sustainable biochar technologies.

In recent years, in the sustainable utilization of biological resources, LBC conversion has made positive progress in preparation technology, conversion mechanism and reactivity exploration. However, because this approach still has certain requirements for environmental pressure and energy support, it is difficult to stably control the yield of different green products during conversion process. Especially in the aspect of material conversion mechanism and the improvement of LBC preparation efficiency, there is still some works worthy of attention by scientists and industries. Therefore, we have proposed a few valuable research contents about LBC here for researchers' reference:

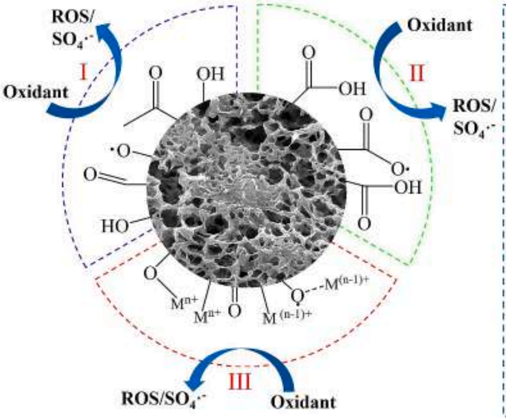

I. $\text{BC surface-OH} + H_2O_2 \rightarrow \cdot OH + H_2O + \text{BC surface-O}\cdot$

$\text{BC surface-OH} + S_2O_8^{2-} \rightarrow SO_4^{\cdot -} + SO_4^{2-} + \text{BC surface-O}\cdot + H^+$

$\text{BC surface-OH} + HSO_5^- \rightarrow \cdot OH/SO_4^{\cdot -} + (SO_4^{2-}+H^+)/H_2O + \text{BC surface-O}\cdot$

$\text{BC surface-OH} + O_2 \rightarrow (\cdot O_2^- + H^+)/(\cdot OOH) + \text{BC surface-O}\cdot$

II. $\text{BC surface-COOH} + H_2O_2 \rightarrow \cdot OH + H_2O + \text{BC surface-COO}\cdot$

$\text{BC surface-COOH} + S_2O_8^{2-} \rightarrow SO_4^{\cdot -} + SO_4^{2-} + \text{BC surface-COO}\cdot + H^+$

$\text{BC surface-COOH} + HSO_5^- \rightarrow \cdot OH/SO_4^{\cdot -} + (SO_4^{2-}+H^+)/H_2O + \text{BC surface-COO}\cdot$

$\text{BC surface-COOH} + O_2 \rightarrow (\cdot O_2^- + H^+)/(\cdot OOH) + \text{BC surface-COO}\cdot$

III. $\text{BC surface-M}^{(n-1)+} + \text{Oxidant} \rightarrow \cdot OH/SO_4^{\cdot -}/\cdot O_2^- + \text{BC surface-M}^{n+}$

$\text{BC surface-O}\cdot\text{- -M}^{(n-1)+} + \text{Oxidant} \rightarrow \cdot OH/SO_4^{\cdot -}/\cdot O_2^- + \text{BC surface=O- -M}^{(n-1)+}$

Other pathways:

i. $\text{BC surface}\cdot + O_2 \rightarrow \text{BC surface-OO}\cdot$, $\text{BC surface-OO}\cdot \xrightarrow{H_2O} \text{BC surface}^+ + \cdot O_2^-$

ii. $\text{BC surface}\cdot + O_2 \rightarrow \text{BC }(O_2)$, $\text{BC }(O_2) \xrightarrow[h\nu]{H_2O} \text{BC surface}\cdot + {}^1O_2$

iii. $\text{BC surface} + O_3 \rightarrow \cdot OH + \text{BC intermediate products}$

Fig. 12. Possible pathways for LBC to promote the production of active species based on its reactivity.

i) During the heating process of LB, various components will enter different phases due to their characteristic properties. Although bio-gas and bio-oil are desirable resources, they will undoubtedly bring negative effects on the production rate and separation cost of LBC products. Effective extraction and separation of resources and energy substances are extremely important for green development. Hence, it is worthwhile to further compare and study the regulation of preparation methods and transformation conditions for achieving directed production of functional LBC. In addition, the economic and technological analysis and ecological effects of its large-scale application should be also revealed more clearly. The comprehensive utilization of life cycle assessments and other related green chemical assessment methods is inevitable in the future improvement and progress of LBC technologies.

ii) Cellulose, hemicellulose and lignin are the main components of LB, and this paper reviewed their carbonization transformation in detail. However, during the practical preparation of LBC, the understanding of the mutual influence among these substances is not very clear, and the study on the molecular and group level is relatively lacking. Studies using in situ monitoring techniques, such as infrared technology, fluorescence monitoring and mass spectrometry may be helpful for synergetic transformation mechanism of components in LB. Moreover, a lot of work needs to be done to reveal the correlation between LB structures and charring reaction. The introduction of typical functional polymerization models of LB will be of great help for the overall simplification of the complexity brought by intermolecular reaction, reflecting the real process of intramolecular transformation in LB. Furthermore, combining molecular simulation to establish a comprehensive kinetic mechanism model for the carbonization of LB may bring deep insights to explore key reaction pathways in this process as well as discover the origin of LBC reactive structure.

iii) LB ash is thought to have impacts on LBC reactivity, such as the presence of HMs associated with the generation of PFRs. There are also many ways to improve the content of AFGs and free radicals on LBC surface, including pre-oxidation, loading and plasma treatment. But effectiveness of these improvement ways is limited and the researches on their modification mechanism are not systematic. Retaining and directly transforming as much LBC with active components as possible in the preparation process is worthy of investigation. Combined with theoretical calculation to guide the synthesis of LBC might provide better ideas.

Declaration of competing interest

The authors declare that they have no known competing financial interests or personal relationships that could have appeared to influence the work reported in this paper.

Acknowledgements

This study was financially supported by the Program for the National Natural Science Foundation of China (52170162, 51809090, U20A20323, 51879101, 51579098, 51521006, 21906049), the Innovation Program of Hunan Province (2021RC3049), the Program for Changjiang Scholars and Innovative Research Team in University (IRT-13R17), the Three Gorges Follow-up Research Project (2017HXXY-05), the National Program for Support of Top-Notch Young Professionals of China (2014), the Program for New Century Excellent Talents in University (NCET-13-0186), the Natural Science Foundation of Hunan Province (2019JJ50077, 2019JJ50046), Changsha Science and Technology Focus on Developing General Project (kq2004024) and the Fundamental Research Funds for the Central Universities (531118010114).

Appendix A. Supplementary data

Supplementary data to this article can be found online at https://doi.org/10.1016/j.rser.2021.112056.

References

[1] He D, Zhang C, Zeng G, Yang Y, Huang D, Wang L, et al. A multifunctional platform by controlling of carbon nitride in the core-shell structure: from design to construction, and catalysis applications. Appl Catal, B 2019;258:117957.

[2] Zhou S, Li L, Wu Y, Zhu S, Zhu N, Bu L, et al. UV365 induced elimination of contaminants of emerging concern in the presence of residual nitrite: roles of reactive nitrogen species. Water Res 2020;178:115829.

[3] He C, Xia W, Zhou C, Huang D, Zhang C, Song B, et al. Rational design to manganese and oxygen co-doped polymeric carbon nitride for efficient nonradical activation of peroxymonosulfate and the mechanism insight. Chem Eng J 2022;430:132751.

[4] Wang W, Niu Q, Zeng G, Zhang C, Huang D, Shao B, et al. 1D porous tubular g-C_3N_4 capture black phosphorus quantum dots as 1D/0D metal-free photocatalysts for oxytetracycline hydrochloride degradation and hexavalent chromium reduction. Appl Catal, B 2020;273:119051.

[5] Zhou Y, Zhang C, Huang D, Wang W, Zhai Y, Liang Q, et al. Structure defined 2D Mo_2C/2Dg-C_3N_4 Van der Waals heterojunction: oriented charge flow in-plane and separation within the interface to collectively promote photocatalytic degradation of pharmaceutical and personal care products. Appl Catal, B 2022;301:120749.

[6] Zhang L, Xu C, Champagne P. Overview of recent advances in thermo-chemical conversion of biomass. Energy Convers Manag 2010;51:969–82.

[7] Liu C, Wang H, Karim AM, Sun J, Wang Y. Catalytic fast pyrolysis of lignocellulosic biomass. Chem Soc Rev 2014;43:7594–623.

[8] Hoang AT, Nizetic S, Ong HC, Chong CT, Atabani AE, Pham VV. Acid-based lignocellulosic biomass biorefinery for bioenergy production: advantages, application constraints, and perspectives. J Environ Manag 2021;296:113194.

[9] Hoang AT, Nižetić S, Ong HC, Mofijur M, Ahmed SF, Ashok B, et al. Insight into the recent advances of microwave pretreatment technologies for the conversion

of lignocellulosic biomass into sustainable biofuel. Chemosphere 2021;281: 130878.

[10] Yang Y, Li X, Zhou C, Xiong W, Zeng G, Huang D, et al. Recent advances in application of graphitic carbon nitride-based catalysts for degrading organic contaminants in water through advanced oxidation processes beyond photocatalysis: a critical review. Water Res 2020;184:116200.

[11] Qin F, Li J, Zhang C, Zeng G, Huang D, Tan X, et al. Biochar in the 21st century: a data-driven visualization of collaboration, frontier identification, and future trend. Sci Total Environ 2021:151774.

[12] Hoang AT, Nižetić S, Cheng CK, Luque R, Thomas S, Banh TL, et al. Heavy metal removal by biomass-derived carbon nanotubes as a greener environmental remediation: a comprehensive review. Chemosphere 2022;287:131959.

[13] Tuan Hoang A, Nižetić S, Ölçer AI, Chyuan Ong H. Synthesis pathway and combustion mechanism of a sustainable biofuel 2,5-Dimethylfuran: progress and prospective. Fuel 2021;286:119337.

[14] Tuan Hoang A, Viet Pham V. 2-Methylfuran (MF) as a potential biofuel: a thorough review on the production pathway from biomass, combustion progress, and application in engines. Renew Sustain Energy Rev 2021;148:111265.

[15] Hoang AT, Ong HC, Fattah IMR, Chong CT, Cheng CK, Sakthivel R, et al. Progress on the lignocellulosic biomass pyrolysis for biofuel production toward environmental sustainability. Fuel Process Technol 2021;223:106997.

[16] Wang S, Dai G, Yang H, Luo Z. Lignocellulosic biomass pyrolysis mechanism: a state-of-the-art review. Prog Energy Combust Sci 2017;62:33–86.

[17] Zhang C, Wang W, Duan A, Zeng G, Huang D, Lai C, et al. Adsorption behavior of engineered carbons and carbon nanomaterials for metal endocrine disruptors: experiments and theoretical calculation. Chemosphere 2019;222:184–94.

[18] Titirici M-M, White RJ, Brun N, Budarin VL, Su DS, del Monte F, et al. Sustainable carbon materials. Chem Soc Rev 2015;44:250–90.

[19] Titirici M-M, White RJ, Falco C, Sevilla M. Black perspectives for a green future: hydrothermal carbons for environment protection and energy storage. Energy Environ Sci 2012;5:6796–822.

[20] Huang C, Zhang C, Huang D, Wang D, Tian S, Wang R, et al. Influence of surface functionalities of pyrogenic carbonaceous materials on the generation of reactive species towards organic contaminants: a review. Chem Eng J 2021;404:127066.

[21] Liu W-J, Jiang H, Yu H-Q. Emerging applications of biochar-based materials for energy storage and conversion. Energy Environ Sci 2019;12:1751–79.

[22] Chen B, Chen Z, Lv S. A novel magnetic biochar efficiently sorbs organic pollutants and phosphate. Bioresour Technol 2011;102:716–23.

[23] Rajapaksha AU, Chen SS, Tsang DCW, Zhang M, Vithanage M, Mandal S, et al. Engineered/designer biochar for contaminant removal/immobilization from soil and water: potential and implication of biochar modification. Chemosphere 2016; 148:276–91.

[24] Xiao L-P, Shi Z-J, Xu F, Sun R-C. Hydrothermal carbonization of lignocellulosic biomass. Bioresour Technol 2012;118:619–23.

[25] Wilk M, Magdziarz A, Jayaraman K, Szymańska-Chargot M, Gökalp I. Hydrothermal carbonization characteristics of sewage sludge and lignocellulosic biomass. A comparative study. Biomass Bioenergy 2019;120:166–75.

[26] Mäkelä M, Benavente V, Fullana A. Hydrothermal carbonization of lignocellulosic biomass: effect of process conditions on hydrochar properties. Appl Energy 2015; 155:576–84.

[27] Su Y, Wen Y, Yang W, Zhang X, Xia M, Zhou N, et al. The mechanism transformation of ramie biochar's cadmium adsorption by aging. Bioresour Technol 2021;330:124947.

[28] Choudhury A, Lansing S. Biochar addition with Fe impregnation to reduce H_2S production from anaerobic digestion. Bioresour Technol 2020;306:123121.

[29] Liu Q, Jiang S, Su X, Zhang X, Cao W, Xu Y. Role of the biochar modified with ZnCl2 and $FeCl_3$ on the electrochemical degradation of nitrobenzene. Chemosphere 2021;275:129966.

[30] Zhao C, Zhong S, Li C, Zhou H, Zhang S. Property and mechanism of phenol degradation by biochar activated persulfate. J Mater Res Technol 2020;9:601–9.

[31] Wu L, Wei C, Zhang S, Wang Y, Kuzyakov Y, Ding X. MgO-modified biochar increases phosphate retention and rice yields in saline-alkaline soil. J Clean Prod 2019;235:901–9.

[32] Liang J, Xu X, Qamar Zaman W, Hu X, Zhao L, Qiu H, et al. Different mechanisms between biochar and activated carbon for the persulfate catalytic degradation of sulfamethoxazole: roles of radicals in solution or solid phase. Chem Eng J 2019; 375:121908.

[33] Sugiarto Y, Sunyoto NMS, Zhu M, Jones I, Zhang D. Effect of biochar addition on microbial community and methane production during anaerobic digestion of food wastes: the role of minerals in biochar. Bioresour Technol 2021;323:124585.

[34] Qiu Z, Chen J, Tang J, Zhang Q. A study of cadmium remediation and mechanisms: improvements in the stability of walnut shell-derived biochar. Sci Total Environ 2018;636:80–4.

[35] Yuan H, Zhang Z, Li M, Clough T, Wrage-Mönnig N, Qin S, et al. Biochar's role as an electron shuttle for mediating soil N_2O emissions. Soil Biol Biochem 2019;133: 94–6.

[36] Yin Z, Xu S, Liu S, Xu S, Li J, Zhang Y. A novel magnetic biochar prepared by K_2FeO_4-promoted oxidative pyrolysis of pomelo peel for adsorption of hexavalent chromium. Bioresour Technol 2020;300:122680.

[37] Tran HN, Tomul F, Thi Hoang Ha N, Nguyen DT, Lima EC, Le GT, et al. Innovative spherical biochar for pharmaceutical removal from water: insight into adsorption mechanism. J Hazard Mater 2020;394:122255.

[38] Hill RA, Hunt J, Sanders E, Tran M, Burk GA, Mlsna TE, et al. Effect of biochar on microbial growth: a metabolomics and bacteriological investigation in E. coli. Environ Sci Technol 2019;53:2635–46.

[39] Ramlow M, Cotrufo MF. Woody biochar's greenhouse gas mitigation potential across fertilized and unfertilized agricultural soils and soil moisture regimes. GCB Bioenergy 2018;10:108–22.

[40] Wu J, Yang J, Feng P, Huang G, Xu C, Lin B. High-efficiency removal of dyes from wastewater by fully recycling litchi peel biochar. Chemosphere 2020;246: 125734.

[41] Zhu K, Wang X, Geng M, Chen D, Lin H, Zhang H. Catalytic oxidation of clofibric acid by peroxydisulfate activated with wood-based biochar: effect of biochar pyrolysis temperature, performance and mechanism. Chem Eng J 2019;374: 1253–63.

[42] Ouyang D, Chen Y, Yan J, Qian L, Han L, Chen M. Activation mechanism of peroxymonosulfate by biochar for catalytic degradation of 1,4-dioxane: important role of biochar defect structures. Chem Eng J 2019;370:614–24.

[43] Zhang P, Sun H, Yu L, Sun T. Adsorption and catalytic hydrolysis of carbaryl and atrazine on pig manure-derived biochars: impact of structural properties of biochars. J Hazard Mater 2013;244–245:217–24.

[44] Huang W, Chen J, Zhang J. Adsorption characteristics of methylene blue by biochar prepared using sheep, rabbit and pig manure. Environ Sci Pollut Res 2018;25:29256–66.

[45] Sun K, Ro K, Guo M, Novak J, Mashayekhi H, Xing B. Sorption of bisphenol A, 17α-ethinyl estradiol and phenanthrene on thermally and hydrothermally produced biochars. Bioresour Technol 2011;102:5757–63.

[46] Yu J, Tang L, Pang Y, Zeng G, Feng H, Zou J, et al. Hierarchical porous biochar from shrimp shell for persulfate activation: a two-electron transfer path and key impact factors. Appl Catal, B 2020;260:118160.

[47] Wang J, Liao Z, Ifthikar J, Shi L, Du Y, Zhu J, et al. Treatment of refractory contaminants by sludge-derived biochar/persulfate system via both adsorption and advanced oxidation process. Chemosphere 2017;185:754–63.

[48] Wang J, Shen M, Gong Q, Wang X, Cai J, Wang S, et al. One-step preparation of ZVI-sludge derived biochar without external source of iron and its application on persulfate activation. Sci Total Environ 2020;714:136728.

[49] Ni B-J, Huang Q-S, Wang C, Ni T-Y, Sun J, Wei W. Competitive adsorption of heavy metals in aqueous solution onto biochar derived from anaerobically digested sludge. Chemosphere 2019;219:351–7.

[50] Kan T, Strezov V, Evans TJ. Lignocellulosic biomass pyrolysis: a review of product properties and effects of pyrolysis parameters. Renew Sustain Energy Rev 2016; 57:1126–40.

[51] Pignatello JJ, Mitch WA, Xu W. Activity and reactivity of pyrogenic carbonaceous matter toward organic compounds. Environ Sci Technol 2017;51:8893–908.

[52] Rubin EM. Genomics of cellulosic biofuels. Nature 2008;454:841–5.

[53] Huang D-L, Zeng G-M, Feng C-L, Hu S, Jiang X-Y, Tang L, et al. Degradation of lead-contaminated lignocellulosic waste by phanerochaete chrysosporium and the reduction of lead toxicity. Environ Sci Technol 2008;42:4946–51.

[54] Gírio FM, Fonseca C, Carvalheiro F, Duarte LC, Marques S, Bogel-Łukasik R. Hemicelluloses for fuel ethanol: a review. Bioresour Technol 2010;101:4775–800.

[55] Liu W-J, Jiang H, Yu H-Q. Thermochemical conversion of lignin to functional materials: a review and future directions. Green Chem 2015;17:4888–907.

[56] Tan H, Li J, He M, Li J, Zhi D, Qin F, et al. Global evolution of research on green energy and environmental technologies:A bibliometric study. J Environ Manag 2021;297:113382.

[57] Titirici M-M, Antonietti M. Chemistry and materials options of sustainable carbon materials made by hydrothermal carbonization. Chem Soc Rev 2010;39:103–16.

[58] Keiluweit M, Nico PS, Johnson MG, Kleber M. Dynamic molecular structure of plant biomass-derived black carbon (biochar). Environ Sci Technol 2010;44: 1247–53.

[59] Chen Z, Chen B, Chiou CT. Fast and slow rates of naphthalene sorption to biochars produced at different temperatures. Environ Sci Technol 2012;46:11104–11.

[60] Meyer S, Glaser B, Quicker P. Technical, economical, and climate-related aspects of biochar production technologies: a literature review. Environ Sci Technol 2011;45:9473–83.

[61] Tripathi M, Sahu JN, Ganesan P. Effect of process parameters on production of biochar from biomass waste through pyrolysis: a review. Renew Sustain Energy Rev 2016;55:467–81.

[62] Mabrouki J, Abbassi MA, Guedri K, Omri A, Jeguirim M. Simulation of biofuel production via fast pyrolysis of palm oil residues. Fuel 2015;159:819–27.

[63] Zhang X, Rajagopalan K, Lei H, Ruan R, Sharma BK. An overview of a novel concept in biomass pyrolysis: microwave irradiation. Sustain Energy Fuels 2017; 1:1664–99.

[64] Liew RK, Nam WL, Chong MY, Phang XY, Su MH, Yek PNY, et al. Oil palm waste: an abundant and promising feedstock for microwave pyrolysis conversion into good quality biochar with potential multi-applications. Process Saf Environ Protect 2018;115:57–69.

[65] Nizamuddin S, Mubarak NM, Tiripathi M, Jayakumar NS, Sahu JN, Ganesan P. Chemical, dielectric and structural characterization of optimized hydrochar produced from hydrothermal carbonization of palm shell. Fuel 2016;163:88–97.

[66] Antal MJ, Mochidzuki K, Paredes LS. Flash carbonization of biomass. Ind Eng Chem Res 2003;42:3690–9.

[67] Heidenreich S, Foscolo PU. New concepts in biomass gasification. Prog Energy Combust Sci 2015;46:72–95.

[68] Hue N. Biochar for maintaining soil health. In: Giri B, Varma A, editors. Soil health. Cham: Springer International Publishing; 2020. p. 21–46.

[69] Kumar A, Saini K, Bhaskar T. Hydochar and biochar: production, physicochemical properties and techno-economic analysis. Bioresour Technol 2020;310:123442.

[70] Manyà JJ. Pyrolysis for biochar purposes: a review to establish current knowledge gaps and research needs. Environ Sci Technol 2012;46:7939–54.

[71] Chen W-H, Peng J, Bi XT. A state-of-the-art review of biomass torrefaction, densification and applications. Renew Sustain Energy Rev 2015;44:847–66.

[72] Uchimiya M, Hiradate S, Antal MJ. Dissolved phosphorus speciation of flash carbonization, slow pyrolysis, and fast pyrolysis biochars. ACS Sustainable Chem Eng 2015;3:1642–9.

[73] Wang R-Z, Huang D-L, Liu Y-G, Zhang C, Lai C, Zeng G-M, et al. Investigating the adsorption behavior and the relative distribution of Cd^{2+} sorption mechanisms on biochars by different feedstock. Bioresour Technol 2018;261:265–71.

[74] Dall'Ora M, Jensen PA, Jensen AD. Suspension combustion of wood: influence of pyrolysis conditions on char yield, morphology, and reactivity. Energy Fuels 2008;22:2955–62.

[75] Mimmo T, Panzacchi P, Baratieri M, Davies CA, Tonon G. Effect of pyrolysis temperature on miscanthus (Miscanthus × giganteus) biochar physical, chemical and functional properties. Biomass Bioenergy 2014;62:149–57.

[76] Manyà JJ, Laguarta S, Ortigosa MA, Manso JA. Biochar from slow pyrolysis of two-phase olive mill waste: effect of pressure and peak temperature on its potential stability. Energy Fuels 2014;28:3271–80.

[77] Melligan F, Auccaise R, Novotny EH, Leahy JJ, Hayes MHB, Kwapinski W. Pressurised pyrolysis of Miscanthus using a fixed bed reactor. Bioresour Technol 2011;102:3466–70.

[78] Manyà JJ, Ortigosa MA, Laguarta S, Manso JA. Experimental study on the effect of pyrolysis pressure, peak temperature, and particle size on the potential stability of vine shoots-derived biochar. Fuel 2014;133:163–72.

[79] Wang L, Ø Skreiberg, Gronli M, Specht GP, Antal MJ. Is elevated pressure required to achieve a high fixed-carbon yield of charcoal from biomass? Part 2: the importance of particle size. Energy Fuels 2013;27:2146–56.

[80] Ge S, Yek PNY, Cheng YW, Xia C, Wan Mahari WA, Liew RK, et al. Progress in microwave pyrolysis conversion of agricultural waste to value-added biofuels: a batch to continuous approach. Renew Sustain Energy Rev 2021;135:110148.

[81] Luque R, Menéndez JA, Arenillas A, Cot J. Microwave-assisted pyrolysis of biomass feedstocks: the way forward? Energy Environ Sci 2012;5:5481–8.

[82] Jones DA, Lelyveld TP, Mavrofidis SD, Kingman SW, Miles NJ. Microwave heating applications in environmental engineering—a review. Resour Conserv Recycl 2002;34:75–90.

[83] Zhang C, Qin D, Zhou Y, Qin F, Wang H, Wang W, et al. Dual optimization approach to Mo single atom dispersed g-C3N4 photocatalyst: morphology and defect evolution. Appl Catal, B 2022;303:120904.

[84] Haeldermans T, Campion L, Kuppens T, Vanreppelen K, Cuypers A, Schreurs S. A comparative techno-economic assessment of biochar production from different residue streams using conventional and microwave pyrolysis. Bioresour Technol 2020;318:124083.

[85] Bergius F. Production of hydrogen from water and coal from cellulose at high temperatures and pressures. J Soc Chem Ind 1913;32:462–7.

[86] Kambo HS, Dutta A. Comparative evaluation of torrefaction and hydrothermal carbonization of lignocellulosic biomass for the production of solid biofuel. Energy Convers Manag 2015;105:746–55.

[87] Li L, Diederick R, Flora JRV, Berge ND. Hydrothermal carbonization of food waste and associated packaging materials for energy source generation. Waste Manag 2013;33:2478–92.

[88] Li Y, Meas A, Shan S, Yang R, Gai X, Wang H, et al. Hydrochars from bamboo sawdust through acid assisted and two-stage hydrothermal carbonization for removal of two organics from aqueous solution. Bioresour Technol 2018;261:257–64.

[89] Titirici M-M, Antonietti M, Baccile N. Hydrothermal carbon from biomass: a comparison of the local structure from poly- to monosaccharides and pentoses/hexoses. Green Chem 2008;10:1204–12.

[90] Hoekman SK, Broch A, Robbins C. Hydrothermal carbonization (HTC) of lignocellulosic biomass. Energy Fuels 2011;25:1802–10.

[91] Lehmann J. A handful of carbon. Nature 2007;447:143–4.

[92] Mumme J, Eckervogt L, Pielert J, Diakité M, Rupp F, Kern J. Hydrothermal carbonization of anaerobically digested maize silage. Bioresour Technol 2011;102:9255–60.

[93] Bai M, Wilske B, Buegger F, Esperschütz J, Kammann CI, Eckhardt C, et al. Degradation kinetics of biochar from pyrolysis and hydrothermal carbonization in temperate soils. Plant Soil 2013;372:375–87.

[94] Liu Z, Zhang F-S, Wu J. Characterization and application of chars produced from pinewood pyrolysis and hydrothermal treatment. Fuel 2010;89:510–4.

[95] Higman C, Tam S. Advances in coal gasification, hydrogenation, and gas treating for the production of chemicals and fuels. Chem Rev 2014;114:1673–708.

[96] Peterson SC, Jackson MA. Simplifying pyrolysis: using gasification to produce corn stover and wheat straw biochar for sorptive and horticultural media. Ind Crop Prod 2014;53:228–35.

[97] Wang D, Jiang P, Zhang H, Yuan W. Biochar production and applications in agro and forestry systems: a review. Sci Total Environ 2020;723:137775.

[98] Massoudi Farid M, Jeong HJ, Hwang J. Co-gasification of coal–biomass blended char with CO_2 and H_2O: effect of partial pressure of the gasifying agent on reaction kinetics. Fuel 2015;162:234–8.

[99] de Lasa H, Salaices E, Mazumder J, Lucky R. Catalytic steam gasification of biomass: catalysts, thermodynamics and kinetics. Chem Rev 2011;111:5404–33.

[100] Camps Arbestain M, Saggar S, Leifeld J. Environmental benefits and risks of biochar application to soil. Agric Ecosyst Environ 2014;191:1–4.

[101] Hajaligol M, Waymack B, Kellogg D. Low temperature formation of aromatic hydrocarbon from pyrolysis of cellulosic materials. Fuel 2001;80:1799–807.

[102] Keiluweit M, Kleber M, Sparrow MA, Simoneit BRT, Prahl FG. Solvent-extractable polycyclic aromatic hydrocarbons in biochar: influence of pyrolysis temperature and feedstock. Environ Sci Technol 2012;46:9333–41.

[103] Hale SE, Lehmann J, Rutherford D, Zimmerman AR, Bachmann RT, Shitumbanuma V, et al. Quantifying the total and bioavailable polycyclic aromatic hydrocarbons and dioxins in biochars. Environ Sci Technol 2012;46:2830–8.

[104] Qian K, Kumar A, Zhang H, Bellmer D, Huhnke R. Recent advances in utilization of biochar. Renew Sustain Energy Rev 2015;42:1055–64.

[105] You S, Ok YS, Chen SS, Tsang DCW, Kwon EE, Lee J, et al. A critical review on sustainable biochar system through gasification: energy and environmental applications. Bioresour Technol 2017;246:242–53.

[106] Wade SR, Nunoura T, Antal MJ. Studies of the flash carbonization process. 2. Violent ignition behavior of pressurized packed beds of biomass:A factorial study. Ind Eng Chem Res 2006;45:3512–9.

[107] Hirst EA, Taylor A, Mokaya R. A simple flash carbonization route for conversion of biomass to porous carbons with high CO_2 storage capacity. J Mater Chem 2018;6:12393–403.

[108] Shabangu S, Woolf D, Fisher EM, Angenent LT, Lehmann J. Techno-economic assessment of biomass slow pyrolysis into different biochar and methanol concepts. Fuel 2014;117:742–8.

[109] Alhashimi HA, Aktas CB. Life cycle environmental and economic performance of biochar compared with activated carbon: a meta-analysis. Resour Conserv Recycl 2017;118:13–26.

[110] Han J, Sen SM, Alonso DM, Dumesic JA, Maravelias CT. A strategy for the simultaneous catalytic conversion of hemicellulose and cellulose from lignocellulosic biomass to liquid transportation fuels. Green Chem 2014;16:653–61.

[111] Mettler MS, Paulsen AD, Vlachos DG, Dauenhauer PJ. Pyrolytic conversion of cellulose to fuels: levoglucosan deoxygenation via elimination and cyclization within molten biomass. Energy Environ Sci 2012;5:7864–8.

[112] Sharma A, Pareek V, Zhang D. Biomass pyrolysis—a review of modelling, process parameters and catalytic studies. Renew Sustain Energy Rev 2015;50:1081–96.

[113] Kilzer FJ, Broido A. Speculation on the nature of cellulose pyrolysis. Pyrodynamics 1965;2:9–18.

[114] Mettler MS, Vlachos DG, Dauenhauer PJ. Top ten fundamental challenges of biomass pyrolysis for biofuels. Energy Environ Sci 2012;5:7797–809.

[115] Mettler MS, Paulsen AD, Vlachos DG, Dauenhauer PJ. Tuning cellulose pyrolysis chemistry: selective decarbonylation via catalyst-impregnated pyrolysis. Catal Sci Technol 2014;4:3822–5.

[116] Falco C, Baccile N, Titirici M-M. Morphological and structural differences between glucose, cellulose and lignocellulosic biomass derived hydrothermal carbons. Green Chem 2011;13:3273–81.

[117] Fu P, Yi W, Bai X, Li Z, Hu S, Xiang J. Effect of temperature on gas composition and char structural features of pyrolyzed agricultural residues. Bioresour Technol 2011;102:8211–9.

[118] Zhou C-H, Xia X, Lin C-X, Tong D-S, Beltramini J. Catalytic conversion of lignocellulosic biomass to fine chemicals and fuels. Chem Soc Rev 2011;40:5588–617.

[119] Zhou X, Li W, Mabon R, Broadbelt LJ. A critical review on hemicellulose pyrolysis. Energy Technol 2017;5:52–79.

[120] Patwardhan PR, Brown RC, Shanks BH. Product distribution from the fast pyrolysis of hemicellulose. ChemSusChem 2011;4:636–43.

[121] Benítez-Guerrero M, López-Beceiro J, Sánchez-Jiménez PE, Pascual-Cosp J. Comparison of thermal behavior of natural and hot-washed sisal fibers based on their main components: cellulose, xylan and lignin. TG-FTIR analysis of volatile products. Thermochim Acta 2014;581:70–86.

[122] Kang S, Li X, Fan J, Chang J. Characterization of hydrochars produced by hydrothermal carbonization of lignin, cellulose, d-xylose, and wood meal. Ind Eng Chem Res 2012;51:9023–31.

[123] Shen D, Zhang L, Xue J, Guan S, Liu Q, Xiao R. Thermal degradation of xylan-based hemicellulose under oxidative atmosphere. Carbohydr Polym 2015;127:363–71.

[124] Couhert C, Commandre J-M, Salvador S. Is it possible to predict gas yields of any biomass after rapid pyrolysis at high temperature from its composition in cellulose, hemicellulose and lignin? Fuel 2009;88:408–17.

[125] Collard F-X, Blin J. A review on pyrolysis of biomass constituents: mechanisms and composition of the products obtained from the conversion of cellulose, hemicelluloses and lignin. Renew Sustain Energy Rev 2014;38:594–608.

[126] Shen DK, Gu S, Bridgwater AV. Study on the pyrolytic behaviour of xylan-based hemicellulose using TG–FTIR and Py–GC–FTIR. J Anal Appl Pyrolysis 2010;87:199–206.

[127] Branca C, Di Blasi C, Mango C, Hrablay I. Products and kinetics of glucomannan pyrolysis. Ind Eng Chem Res 2013;52:5030–9.

[128] Zakzeski J, Bruijnincx PCA, Jongerius AL, Weckhuysen BM. The catalytic valorization of lignin for the production of renewable chemicals. Chem Rev 2010;110:3552–99.

[129] Akazawa M, Kojima Y, Kato Y. Effect of pyrolysis temperature on the pyrolytic degradation mechanism of β-aryl ether linkages. J Anal Appl Pyrolysis 2016;118:164–74.

[130] Kawamoto H. Lignin pyrolysis reactions. J Wood Sci 2017;63:117–32.

[131] Asmadi M, Kawamoto H, Saka S. Thermal reactions of guaiacol and syringol as lignin model aromatic nuclei. J Anal Appl Pyrolysis 2011;92:88–98.

[132] Asmadi M, Kawamoto H, Saka S. Thermal reactivities of catechols/pyrogallols and cresols/xylenols as lignin pyrolysis intermediates. J Anal Appl Pyrolysis 2011;92:76–87.

[133] Huang J, Li X, Wu D, Tong H, Li W. Theoretical studies on pyrolysis mechanism of guaiacol as lignin model compound. J Renew Sustain Energy 2013;5:043112.

[134] Liu C, Zhang Y, Huang X. Study of guaiacol pyrolysis mechanism based on density function theory. Fuel Process Technol 2014;123:159–65.

[135] Liu C, Deng Y, Wu S, Mou H, Liang J, Lei M. Study on the pyrolysis mechanism of three guaiacyl-type lignin monomeric model compounds. J Anal Appl Pyrolysis 2016;118:123–9.

[136] Wang M, Liu C, Xu X, Li Q. Theoretical study of the pyrolysis of vanillin as a model of secondary lignin pyrolysis. Chem Phys Lett 2016;654:41–5.

[137] Chakar FS, Ragauskas AJ. Review of current and future softwood kraft lignin process chemistry. Ind Crop Prod 2004;20:131–41.

[138] Chu S, Subrahmanyam AV, Huber GW. The pyrolysis chemistry of a β-O-4 type oligomeric lignin model compound. Green Chem 2013;15:125–36.

[139] Cho J, Chu S, Dauenhauer PJ, Huber GW. Kinetics and reaction chemistry for slow pyrolysis of enzymatic hydrolysis lignin and organosolv extracted lignin derived from maplewood. Green Chem 2012;14:428–39.

[140] Hosoya T, Kawamoto H, Saka S. Pyrolysis gasification reactivities of primary tar and char fractions from cellulose and lignin as studied with a closed ampoule reactor. J Anal Appl Pyrolysis 2008;83:71–7.

[141] Li C, Zhao X, Wang A, Huber GW, Zhang T. Catalytic transformation of lignin for the production of chemicals and fuels. Chem Rev 2015;115:11559–624.

[142] Huang X, Liu C, Huang J, Li H. Theory studies on pyrolysis mechanism of phenethyl phenyl ether. Comput Theor Chem 2011;976:51–9.

[143] Huang J, Liu C, Wu D, Tong H, Ren L. Density functional theory studies on pyrolysis mechanism of β-O-4 type lignin dimer model compound. J Anal Appl Pyrolysis 2014;109:98–108.

[144] Elder T, Beste A. Density functional theory study of the concerted pyrolysis mechanism for lignin models. Energy Fuels 2014;28:5229–35.

[145] Song Y, Zhang J, Zhang X, Tan T. The correlation between cellulose allomorphs (I and II) and conversion after removal of hemicellulose and lignin of lignocellulose. Bioresour Technol 2015;193:164–70.

[146] da Silva Lacerda V, López-Sotelo JB, Correa-Guimarães A, Hernández-Navarro S, Sánchez-Bascones M, Navas-Gracia LM, et al. A kinetic study on microwave-assisted conversion of cellulose and lignocellulosic waste into hydroxymethylfurfural/furfural. Bioresour Technol 2015;180:88–96.

[147] Nieva ML, Volpe MA, Moyano EL. Catalytic and catalytic free process for cellulose conversion: fast pyrolysis and microwave induced pyrolysis studies. Cellulose 2015;22:215–28.

[148] Vispute TP, Zhang H, Sanna A, Xiao R, Huber GW. Renewable chemical commodity feedstocks from integrated catalytic processing of pyrolysis oils. Science 2010;330:1222.

[149] Zhang C, Lai C, Zeng G, Huang D, Yang C, Wang Y, et al. Efficacy of carbonaceous nanocomposites for sorbing ionizable antibiotic sulfamethazine from aqueous solution. Water Res 2016;95:103–12.

[150] Carlson TR, Cheng Y-T, Jae J, Huber GW. Production of green aromatics and olefins by catalytic fast pyrolysis of wood sawdust. Energy Environ Sci 2011;4:145–61.

[151] Liu W-J, Jiang H, Yu H-Q. Development of biochar-based functional materials: toward a sustainable platform carbon. Mater Chem Rev 2015;115:12251–85.

[152] Du S, Valla JA, Bollas GM. Characteristics and origin of char and coke from fast and slow, catalytic and thermal pyrolysis of biomass and relevant model compounds. Green Chem 2013;15:3214–29.

[153] Caeiro G, Lopes JM, Magnoux P, Ayrault P, Ramôa Ribeiro F. A FT-IR study of deactivation phenomena during methylcyclohexane transformation on H-USY zeolites: nitrogen poisoning, coke formation, and acidity–activity correlations. J Catal 2007;249:234–43.

[154] Jae J, Tompsett GA, Foster AJ, Hammond KD, Auerbach SM, Lobo RF, et al. Investigation into the shape selectivity of zeolite catalysts for biomass conversion. J Catal 2011;279:257–68.

[155] Chen Y, Yang H, Wang X, Zhang S, Chen H. Biomass-based pyrolytic polygeneration system on cotton stalk pyrolysis: influence of temperature. Bioresour Technol 2012;107:411–8.

[156] Lian F, Xing B. Black carbon (biochar) in water/soil environments: molecular structure, sorption, stability, and potential risk. Environ Sci Technol 2017;51:13517–32.

[157] Sun K, Kang M, Ro KS, Libra JA, Zhao Y, Xing B. Variation in sorption of propiconazole with biochars: the effect of temperature, mineral, molecular structure, and nano-porosity. Chemosphere 2016;142:56–63.

[158] Singh BP, Cowie AL, Smernik RJ. Biochar carbon stability in a clayey soil as a function of feedstock and pyrolysis temperature. Environ Sci Technol 2012;46:11770–8.

[159] Xiao X, Chen B. A direct observation of the fine aromatic clusters and molecular structures of biochars. Environ Sci Technol 2017;51:5473–82.

[160] Wang J, Wang S. Preparation, modification and environmental application of biochar: a review. J Clean Prod 2019;227:1002–22.

[161] Babeł K, Jurewicz K. KOH activated lignin based nanostructured carbon exhibiting high hydrogen electrosorption. Carbon 2008;46:1948–56.

[162] Lua AC, Yang T, Guo J. Effects of pyrolysis conditions on the properties of activated carbons prepared from pistachio-nut shells. J Anal Appl Pyrolysis 2004;72:279–87.

[163] Lehmann J, Joseph S. Biochar for environmental management. 2009.

[164] Brewer CE, Schmidt-Rohr K, Satrio JA, Brown RC. Characterization of biochar from fast pyrolysis and gasification systems. Environ Prog Sustain Energy 2009;28:386–96.

[165] Cao X, Pignatello JJ, Li Y, Lattao C, Chappell MA, Chen N, et al. Characterization of wood chars produced at different temperatures using advanced solid-state ^{13}C NMR spectroscopic techniques. Energy Fuels 2012;26:5983–91.

[166] Xiao X, Chen Z, Chen B. H/C atomic ratio as a smart linkage between pyrolytic temperatures, aromatic clusters and sorption properties of biochars derived from diverse precursory materials. Sci Rep 2016;6:22644.

[167] Wiedemeier DB, Abiven S, Hockaday WC, Keiluweit M, Kleber M, Masiello CA, et al. Aromaticity and degree of aromatic condensation of char. Org Geochem 2015;78:135–43.

[168] Heymann K, Lehmann J, Solomon D, Schmidt MWI, Regier T. C 1s K-edge near edge X-ray absorption fine structure (NEXAFS) spectroscopy for characterizing functional group chemistry of black carbon. Org Geochem 2011;42:1055–64.

[169] Xiao X, Chen B, Chen Z, Zhu L, Schnoor JL. Insight into multiple and multilevel structures of biochars and their potential environmental applications: a critical review. Environ Sci Technol 2018;52:5027–47.

[170] Saletnik B. Biochar as a multifunctional component of the environment-A review. Appl Sci 2019;9:1139.

[171] Nguyen BT, Lehmann J, Hockaday WC, Joseph S, Masiello CA. Temperature sensitivity of black carbon decomposition and oxidation. Environ Sci Technol 2010;44:3324–31.

[172] Chen B, Zhou D, Zhu L. Transitional adsorption and partition of nonpolar and polar aromatic contaminants by biochars of pine needles with different pyrolytic temperatures. Environ Sci Technol 2008;42:5137–43.

[173] Leng L, Huang H. An overview of the effect of pyrolysis process parameters on biochar stability. Bioresour Technol 2018;270:627–42.

[174] Rocca PAD, Cerrella EG, Bonelli PR, Cukierman AL. Pyrolysis of hardwoods residues: on kinetics and chars characterization. Biomass Bioenergy 1999;16:79–88.

[175] Czernik S, Bridgwater AV. Overview of applications of biomass fast pyrolysis oil. Energy Fuels 2004;18:590–8.

[176] Prakongkep N. The effects of pyrolysis conditions on the chemical and physical properties of rice husk biochar. Int J Mater Sci 2013;3:98–103.

[177] Wang Z, Liu G, Zheng H, Li F, Ngo HH, Guo W, et al. Investigating the mechanisms of biochar's removal of lead from solution. Bioresour Technol 2015;177:308–17.

[178] Freitas JCC, Emmerich FG, Bonagamba TJ. High-resolution solid-state NMR study of the occurrence and thermal transformations of silicon-containing species in biomass materials. Chem Mater 2000;12:711–8.

[179] Shen Y, Zhao P, Shao Q, Ma D, Takahashi F, Yoshikawa K. In-situ catalytic conversion of tar using rice husk char-supported nickel-iron catalysts for biomass pyrolysis/gasification. Appl Catal, B 2014;152–153:140–51.

[180] Xiao X, Chen B, Zhu L. Transformation, morphology, and dissolution of silicon and carbon in rice straw-derived biochars under different pyrolytic temperatures. Environ Sci Technol 2014;48:3411–9.

[181] Sun L, Tian C, Li M, Meng X, Wang L, Wang R, et al. From coconut shell to porous graphene-like nanosheets for high-power supercapacitors. J Mater Chem 2013;1:6462–70.

[182] Liu W-J, Jiang H, Tian K, Ding Y-W, Yu H-Q. Mesoporous carbon stabilized MgO nanoparticles synthesized by pyrolysis of $MgCl_2$ preloaded waste biomass for highly efficient CO_2 capture. Environ Sci Technol 2013;47:9397–403.

[183] Vijayaraghavan K. The importance of mineral ingredients in biochar production, properties and applications. Crit Rev Environ Sci Technol 2021;51:113–39.

[184] Yan Q, Wan C, Liu J, Gao J, Yu F, Zhang J, et al. Iron nanoparticles in situ encapsulated in biochar-based carbon as an effective catalyst for the conversion of biomass-derived syngas to liquid hydrocarbons. Green Chem 2013;15:1631–40.

[185] Wu H, Feng Q, Lu P, Chen M, Yang H. Degradation mechanisms of cefotaxime using biochar supported Co/Fe bimetallic nanoparticles. Environ Sci: Water Res Technol 2018;4:964–75.

[186] Deng J, Dong H, Zhang C, Jiang Z, Cheng Y, Hou K, et al. Nanoscale zero-valent iron/biochar composite as an activator for Fenton-like removal of sulfamethazine. Separ Purif Technol 2018;202:130–7.

[187] Chen Z, Xiao X, Chen B, Zhu L. Quantification of chemical states, dissociation constants and contents of oxygen-containing groups on the surface of biochars produced at different temperatures. Environ Sci Technol 2015;49:309–17.

[188] Liu W-J, Li W-W, Jiang H, Yu H-Q. Fates of chemical elements in biomass during its pyrolysis. Chem Rev 2017;117:6367–98.

[189] Sun K, Kang M, Zhang Z, Jin J, Wang Z, Pan Z, et al. Impact of deashing treatment on biochar structural properties and potential sorption mechanisms of phenanthrene. Environ Sci Technol 2013;47:11473–81.

[190] Nguyen BT, Lehmann J. Black carbon decomposition under varying water regimes. Org Geochem 2009;40:846–53.

[191] Schmidt H-P, Abiven S, Kammann C, Glaser B, Bucheli T, Leifeld J, et al. European biochar certificate - guidelines for a sustainable production of biochar. 2013.

[192] Spokas KA. Review of the stability of biochar in soils: predictability of O:C molar ratios. Carbon Manag 2010;1:289–303.

[193] Wang T, Camps-Arbestain M, Hedley M, Singh BP, Calvelo-Pereira R, Wang C. Determination of carbonate-C in biochars. Soil Res 2014;52:495–504.

[194] Abdullah H, Wu H. Biochar as a fuel: 1. Properties and grindability of biochars produced from the pyrolysis of mallee wood under slow-heating conditions. Energy Fuels 2009;23:4174–81.

[195] Schindler DW, Hecky RE. Eutrophication: more nitrogen data needed. Science 2009;324:721.

[196] Bulen W, Burns R, Lecomte J. Nitrogen fixation: hydrosulfite as electron donor with cell-free preparations of Azotobacter vinelandii and Rhodospirillum rubrum. Proc Natl Acad Sci U S A 1965;53:532–9.

[197] Iamchaturapatr J, Yi SW, Rhee JS. Nutrient removals by 21 aquatic plants for vertical free surface-flow (VFS) constructed wetland. Ecol Eng 2007;29:287–93.

[198] Nanda S, Mohanty P, Pant KK, Naik S, Kozinski JA, Dalai AK. Characterization of north American lignocellulosic biomass and biochars in terms of their candidacy for alternate renewable fuels. BioEnergy Res 2013;6:663–77.
[199] Knicker H, Hilscher A, González-Vila FJ, Almendros G. A new conceptual model for the structural properties of char produced during vegetation fires. Org Geochem 2008;39:935–9.
[200] Liu L, Tan Z, Gong H, Huang Q. Migration and transformation mechanisms of nutrient elements (N, P, K) within biochar in straw–biochar–soil–plant systems: a review. ACS Sustainable Chem Eng 2019;7:22–32.
[201] Tack FMG, Rinklebe J, Ok YS. Interactions between biochar and trace elements in the environment. Sci Total Environ 2019;649:792.
[202] Li L, Jia C, Zhu X, Zhang S. Utilization of cigarette butt waste as functional carbon precursor for supercapacitors and adsorbents. J Clean Prod 2020;256:120326.
[203] Zhu S, Huang X, Ma F, Wang L, Duan X, Wang S. Catalytic removal of aqueous contaminants on N-doped graphitic biochars: inherent roles of adsorption and nonradical mechanisms. Environ Sci Technol 2018;52:8649–58.
[204] Gao K, Wang B, Tao L, Cunning BV, Zhang Z, Wang S, et al. Efficient metal-free electrocatalysts from N-doped carbon nanomaterials: mono-doping and Co-doping. Adv Mater 2019;31:1805121.
[205] Guo D, Shibuya R, Akiba C, Saji S, Kondo T, Nakamura J. Active sites of nitrogen-doped carbon materials for oxygen reduction reaction clarified using model catalysts. Science 2016;351:361–5.
[206] Ma JF, Takahashi E. Chapter 5 - silicon-accumulating plants in the plant kingdom. In: Ma JF, Takahashi E, editors. Soil, fertilizer, and plant silicon research in Japan. Amsterdam: Elsevier Science; 2002.
[207] Ma JF, Takahashi E. Chapter 6 - silicon uptake and accumulation in plants. In: Ma JF, Takahashi E, editors. Soil, fertilizer, and plant silicon research in Japan. Amsterdam: Elsevier Science; 2002.
[208] Schroeder MS, Janos DP. Plant growth, phosphorus nutrition, and root morphological responses to arbuscular mycorrhizas, phosphorus fertilization, and intraspecific density. Mycorrhiza 2005;15:203–16.
[209] Richardson AE, Barea J-M, McNeill AM, Prigent-Combaret C. Acquisition of phosphorus and nitrogen in the rhizosphere and plant growth promotion by microorganisms. Plant Soil 2009;321:305–39.
[210] Uchimiya M, Hiradate S. Pyrolysis temperature-dependent changes in dissolved phosphorus speciation of plant and manure biochars. J Agric Food Chem 2014;62:1802–9.
[211] Cantrell KB, Hunt PG, Uchimiya M, Novak JM, Ro KS. Impact of pyrolysis temperature and manure source on physicochemical characteristics of biochar. Bioresour Technol 2012;107:419–28.
[212] Xu G, Zhang Y, Shao H, Sun J. Pyrolysis temperature affects phosphorus transformation in biochar: chemical fractionation and ^{31}P NMR analysis. Sci Total Environ 2016;569–570:65–72.
[213] Angst TE, Sohi SP. Establishing release dynamics for plant nutrients from biochar. GCB Bioenergy 2013;5:221–6.
[214] Qian T-T, Li D-C, Jiang H. Thermochemical behavior of tris(2-butoxyethyl) phosphate (TBEP) during Co-pyrolysis with biomass. Environ Sci Technol 2014;48:10734–42.
[215] Savant NK, Datnoff LE, Snyder GH. Depletion of plant-available silicon in soils: a possible cause of declining rice yields. Commun Soil Sci Plant Anal 1997;28:1245–52.
[216] Detmann K, Araújo W, Martins S, Sanglard L, Reis J, Detmann E, et al. Silicon nutrition increases grain yield, which, in turn, exerts a feed-forward stimulation of photosynthetic rates via enhanced mesophyll conductance and alters primary metabolism in rice. New Phytol 2012;196:752–62.
[217] Epstein E. Silicon: its manifold roles in plants. Ann Appl Biol 2009;155:155–60.
[218] Ma JF, Takahashi E. Chapter 7 - functions of silicon in plant growth. In: Ma JF, Takahashi E, editors. Soil, fertilizer, and plant silicon research in Japan. Amsterdam: Elsevier Science; 2002.
[219] Liang Y, Nikolic M, Bélanger R, Gong H, Song A. Silicon biogeochemistry and bioavailability in soil. In: Liang Y, Nikolic M, Bélanger R, Gong H, Song A, editors. Silicon in agriculture: from theory to practice. Dordrecht: Springer Netherlands; 2015. p. 45–68.
[220] Qian L, Chen B. Dual role of biochars as adsorbents for aluminum: the effects of oxygen-containing organic components and the scattering of silicate particles. Environ Sci Technol 2013;47:8759–68.
[221] Okuno T, Sonoyama N, Hayashi J-i, Li C-Z, Sathe C, Chiba T. Primary release of alkali and alkaline earth metallic species during the pyrolysis of pulverized biomass. Energy Fuels 2005;19:2164–71.
[222] Keller C, Ludwig C, Davoli F, Wochele J. Thermal treatment of metal-enriched biomass produced from heavy metal phytoextraction. Environ Sci Technol 2005;39:3359–67.
[223] Wang J, Chen C. Biosorbents for heavy metals removal and their future. Biotechnol Adv 2009;27:195–226.
[224] Koppolu L, Prasad R, Davis Clements L. Pyrolysis as a technique for separating heavy metals from hyperaccumulators. Part III: pilot-scale pyrolysis of synthetic hyperaccumulator biomass. Biomass Bioenergy 2004;26:463–72.
[225] Pi Z, Li X, Wang D, Xu Q, Tao Z, Huang X, et al. Persulfate activation by oxidation biochar supported magnetite particles for tetracycline removal: performance and degradation pathway. J Clean Prod 2019;235:1103–15.
[226] Fang G, Gao J, Liu C, Dionysiou DD, Wang Y, Zhou D. Key role of persistent free radicals in hydrogen peroxide activation by biochar: implications to organic contaminant degradation. Environ Sci Technol 2014;48:1902–10.
[227] Gupta VK, Moradi O, Tyagi I, Agarwal S, Sadegh H, Shahryari-Ghoshekandi R, et al. Study on the removal of heavy metal ions from industry waste by carbon nanotubes: effect of the surface modification: a review. Crit Rev Environ Sci Technol 2016;46:93–118.
[228] O'Connor D, Peng T, Li G, Wang S, Duan L, Mulder J, et al. Sulfur-modified rice husk biochar: a green method for the remediation of mercury contaminated soil. Sci Total Environ 2018;621:819–26.
[229] Kasnejad MH, Esfandiari A, Kaghazchi T, Asasian N. Effect of pre-oxidation for introduction of nitrogen containing functional groups into the structure of activated carbons and its influence on Cu (II) adsorption. J Taiwan Inst Chem Eng 2012;43:736–40.
[230] Liao S, Pan B, Li H, Zhang D, Xing B. Detecting free radicals in biochars and determining their ability to inhibit the germination and growth of corn, wheat and rice seedlings. Environ Sci Technol 2014;48:8581–7.
[231] Fang G, Liu C, Gao J, Dionysiou DD, Zhou D. Manipulation of persistent free radicals in biochar to activate persulfate for contaminant degradation. Environ Sci Technol 2015;49:5645–53.
[232] Yang J, Pan B, Li H, Liao S, Zhang D, Wu M, et al. Degradation of p-nitrophenol on biochars: role of persistent free radicals. Environ Sci Technol 2016;50:694–700.
[233] Du L, Xu W, Liu S, Li X, Huang D, Tan X, et al. Activation of persulfate by graphitized biochar for sulfamethoxazole removal: the roles of graphitic carbon structure and carbonyl group. J Colloid Interface Sci 2020;577:419–30.
[234] Zhao Y, Song M, Cao Q, Sun P, Chen Y, Meng F. The superoxide radicals' production via persulfate activated with $CuFe_2O_4$@Biochar composites to promote the redox pairs cycling for efficient degradation of o-nitrochlorobenzene in soil. J Hazard Mater 2020;400:122887.
[235] Jin Z, Xiao S, Dong H, Xiao J, Tian R, Chen J, et al. Adsorption and catalytic degradation of organic contaminants by biochar: overlooked role of biochar's particle size. J Hazard Mater 2022;422:126928.
[236] Hung C-M, Chen C-W, Huang C-P, Shiung Lam S, Dong C-D. Peroxymonosulfate activation by a metal-free biochar for sulfonamide antibiotic removal in water and associated bacterial community composition. Bioresour Technol 2022;343:126082.
[237] Wang H, Guo W, Liu B, Wu Q, Luo H, Zhao Q, et al. Edge-nitrogenated biochar for efficient peroxydisulfate activation: an electron transfer mechanism. Water Res 2019;160:405–14.
[238] Ye S, Zeng G, Tan X, Wu H, Liang J, Song B, et al. Nitrogen-doped biochar fiber with graphitization from Boehmeria nivea for promoted peroxymonosulfate activation and non-radical degradation pathways with enhancing electron transfer. Appl Catal, B 2020;269:118850.
[239] Xu L, Wu C, Liu P, Bai X, Du X, Jin P, et al. Peroxymonosulfate activation by nitrogen-doped biochar from sawdust for the efficient degradation of organic pollutants. Chem Eng J 2020;387:124065.
[240] Ding D, Yang S, Qian X, Chen L, Cai T. Nitrogen-doping positively whilst sulfur-doping negatively affect the catalytic activity of biochar for the degradation of organic contaminant. Appl Catal, B 2020;263:118348.
[241] Oh W-D, Zaeni JRJ, Lisak G, Lin K-YA, Leong K-H, Choong Z-Y. Accelerated organics degradation by peroxymonosulfate activated with biochar co-doped with nitrogen and sulfur. Chemosphere 2021;277:130313.
[242] Xu Y, Liu S, Wang M, Zhang J, Ding H, Song Y, et al. Thiourea-assisted one-step fabrication of a novel nitrogen and sulfur co-doped biochar from nanocellulose as metal-free catalyst for efficient activation of peroxymonosulfate. J Hazard Mater 2021;416:125796.
[243] Huang D, Luo H, Zhang C, Zeng G, Lai C, Cheng M, et al. Nonnegligible role of biomass types and its compositions on the formation of persistent free radicals in biochar: insight into the influences on Fenton-like process. Chem Eng J 2019;361:353–63.
[244] Li L, Lai C, Huang F, Cheng M, Zeng G, Huang D, et al. Degradation of naphthalene with magnetic bio-char activate hydrogen peroxide: synergism of bio-char and Fe–Mn binary oxides. Water Res 2019;160:238–48.
[245] Wang X, Zhang P, Wang C, Jia H, Shang X, Tang J, et al. Metal-rich hyperaccumulator-derived biochar as an efficient persulfate activator: role of intrinsic metals (Fe, Mn and Zn) in regulating characteristics, performance and reaction mechanisms. J Hazard Mater 2022;424:127225.
[246] Yu L, Yuan Y, Tang J, Wang Y, Zhou S. Biochar as an electron shuttle for reductive dechlorination of pentachlorophenol by Geobacter sulfurreducens. Sci Rep 2015;5:16221.
[247] Huang H, Guo T, Wang K, Li Y, Zhang G. Efficient activation of persulfate by a magnetic recyclable rape straw biochar catalyst for the degradation of tetracycline hydrochloride in water. Sci Total Environ 2021;758:143957.
[248] Zhang Y, Xu X, Zhang P, Ling Z, Qiu H, Cao X. Pyrolysis-temperature depended quinone and carbonyl groups as the electron accepting sites in barley grass derived biochar. Chemosphere 2019;232:273–80.
[249] Wu S, Fang G, Wang Y, Zheng Y, Wang C, Zhao F, et al. Redox-active oxygen-containing functional groups in activated carbon facilitate microbial reduction of ferrihydrite. Environ Sci Technol 2017;51:9709–17.
[250] Wang Y, Ao Z, Sun H, Duan X, Wang S. Activation of peroxymonosulfate by carbonaceous oxygen groups: experimental and density functional theory calculations. Appl Catal, B 2016;198:295–302.
[251] Duan X, Sun H, Ao Z, Zhou L, Wang G, Wang S. Unveiling the active sites of graphene-catalyzed peroxymonosulfate activation. Carbon 2016;107:371–8.
[252] Zhou Y, Jiang J, Gao Y, Ma J, Pang S-Y, Li J, et al. Activation of peroxymonosulfate by benzoquinone: a novel nonradical oxidation process. Environ Sci Technol 2015;49:12941–50.
[253] Zhou Y, Jiang J, Gao Y, Pang S-Y, Yang Y, Ma J, et al. Activation of peroxymonosulfate by phenols: important role of quinone intermediates and involvement of singlet oxygen. Water Res 2017;125:209–18.

[254] Harvey OR, Herbert BE, Kuo L-J, Louchouarn P. Generalized two-dimensional perturbation correlation infrared spectroscopy reveals mechanisms for the development of surface charge and recalcitrance in plant-derived biochars. Environ Sci Technol 2012;46:10641–50.

[255] Uchimiya M, Bannon DI, Wartelle LH. Retention of heavy metals by carboxyl functional groups of biochars in small arms range soil. J Agric Food Chem 2012;60:1798–809.

[256] Chen M, Wang F, Zhang D-l, Yi W-m, Liu Y. Effects of acid modification on the structure and adsorption NH4+-N properties of biochar. Renew Energy 2021;169:1343–50.

[257] Li L-x, Li F. The effect of carbonyl, carboxyl and hydroxyl groups on the capacitance of carbon nanotubes. New Carbon Mater 2011;26:224–8.

[258] Li B, Yang L, Wang C-q, Zhang Q-p, Liu Q-c, Li Y-d, et al. Adsorption of Cd(II) from aqueous solutions by rape straw biochar derived from different modification processes. Chemosphere 2017;175:332–40.

[259] Yang X, Wan Y, Zheng Y, He F, Yu Z, Huang J, et al. Surface functional groups of carbon-based adsorbents and their roles in the removal of heavy metals from aqueous solutions: a critical review. Chem Eng J 2019;366:608–21.

[260] Leng L, Xu S, Liu R, Yu T, Zhuo X, Leng S, et al. Nitrogen containing functional groups of biochar: an overview. Bioresour Technol 2020;298:122286.

[261] Guo D, Shibuya R, Akiba C, Saji S, Kondo T, Nakamura J. Active sites of nitrogen-doped carbon materials for oxygen reduction reaction clarified using model catalysts. Science 2016;351:361.

[262] Shen W, Fan W. Nitrogen-containing porous carbons: synthesis and application. J Mater Chem 2013;1:999–1013.

[263] Li K, Cao J, Li H, Liu J, Lu M, Tang D. Nitrogen functionalized hierarchical microporous/mesoporous carbon with a high surface area and controllable nitrogen content for enhanced lead(ii) adsorption. RSC Adv 2016;6:92186–96.

[264] Wang G, Chen S, Quan X, Yu H, Zhang Y. Enhanced activation of peroxymonosulfate by nitrogen doped porous carbon for effective removal of organic pollutants. Carbon 2017;115:730–9.

[265] Pan X, Chen J, Wu N, Qi Y, Xu X, Ge J, et al. Degradation of aqueous 2,4,4′-Trihydroxybenzophenone by persulfate activated with nitrogen doped carbonaceous materials and the formation of dimer products. Water Res 2018;143:176–87.

[266] Zhang H, Wang T, Sui Z, Zhang Y, Sun B, Pan W-P. Enhanced mercury removal by transplanting sulfur-containing functional groups to biochar through plasma. Fuel 2019;253:703–12.

[267] Squadrito GL, Cueto R, Dellinger B, Pryor WA. Quinoid redox cycling as a mechanism for sustained free radical generation by inhaled airborne particulate matter. Free Radical Biol Med 2001;31:1132–8.

[268] Vejerano E, Lomnicki S, Dellinger B. formation and stabilization of combustion-generated environmentally persistent free radicals on an Fe(III)$_2$O$_3$/silica surface. Environ Sci Technol 2011;45:589–94.

[269] Cruz ALNd, Cook RL, Lomnicki SM, Dellinger B. Effect of low temperature thermal treatment on soils contaminated with pentachlorophenol and environmentally persistent free radicals. Environ Sci Technol 2012;46:5971–8.

[270] Zhang C, Zeng G, Huang D, Lai C, Chen M, Cheng M, et al. Biochar for environmental management: mitigating greenhouse gas emissions, contaminant treatment, and potential negative impacts. Chem Eng J 2019;373:902–22.

[271] Zhang Y, Xu M, Liu X, Wang M, Zhao J, Li S, et al. Regulation of biochar mediated catalytic degradation of quinolone antibiotics: important role of environmentally persistent free radicals. Bioresour Technol 2021;326:124780.

[272] Zhang X, Sun P, Wei K, Huang X, Zhang X. Enhanced H$_2$O$_2$ activation and sulfamethoxazole degradation by Fe-impregnated biochar. Chem Eng J 2020;385:123921.

[273] Luo K, Yang Q, Pang Y, Wang D, Li X, Lei M, et al. Unveiling the mechanism of biochar-activated hydrogen peroxide on the degradation of ciprofloxacin. Chem Eng J 2019;374:520–30.

[274] Xiang L, Liu S, Ye S, Yang H, Song B, Qin F, et al. Potential hazards of biochar: the negative environmental impacts of biochar applications. J Hazard Mater 2021;420:126611.

[275] Mendonça FGd, Cunha ITd, Soares RR, Tristão JC, Lago RM. Tuning the surface properties of biochar by thermal treatment. Bioresour Technol 2017;246:28–33.

[276] Uchimiya M, Noda I, Orlov A, Ramakrishnan G. In situ and ex situ 2D infrared/fluorescence correlation monitoring of surface functionality and electron density of biochars. ACS Sustainable Chem Eng 2018;6:8055–62.

[277] Deng R, Luo H, Huang D, Zhang C. Biochar-mediated Fenton-like reaction for the degradation of sulfamethazine: role of environmentally persistent free radicals. Chemosphere 2020;255:126975.

[278] Rivera-Utrilla J, Sánchez-Polo M, Gómez-Serrano V, Álvarez PM, Alvim-Ferraz MCM, Dias JM. Activated carbon modifications to enhance its water treatment applications. An overview. J Hazard Mater 2011;187:1–23.

[279] Li X, Zhou H, Wu W, Wei S, Xu Y, Kuang Y. Studies of heavy metal ion adsorption on Chitosan/Sulfydryl-functionalized graphene oxide composites. J Colloid Interface Sci 2015;448:389–97.

[280] Wang S, Ai S, Nzediegwu C, Kwak J-H, Islam MS, Li Y, et al. Carboxyl and hydroxyl groups enhance ammonium adsorption capacity of iron (III) chloride and hydrochloric acid modified biochars. Bioresour Technol 2020;309:123390.

[281] Odinga ES, Waigi MG, Gudda FO, Wang J, Yang B, Hu X, et al. Occurrence, formation, environmental fate and risks of environmentally persistent free radicals in biochars. Environ Int 2020;134:105172.

[282] Tian S, Zhang C, Huang D, Wang R, Zeng G, Yan M, et al. Recent progress in sustainable technologies for adsorptive and reactive removal of sulfonamides. Chem Eng J 2020;389:123423.

[283] Shrestha PM, Rotaru A-E. Plugging in or going wireless: strategies for interspecies electron transfer. Front Microbiol 2014;5.

[284] Wang B, Wang Z, Jiang Y, Tan G, Xu N, Xu Y. Enhanced power generation and wastewater treatment in sustainable biochar electrodes based bioelectrochemical system. Bioresour Technol 2017;241:841–8.

[285] Cheng B-H, Zeng RJ, Jiang H. Recent developments of post-modification of biochar for electrochemical energy storage. Bioresour Technol 2017;246:224–33.

[286] Genovese M, Jiang J, Lian K, Holm N. High capacitive performance of exfoliated biochar nanosheets from biomass waste corn cob. J Mater Chem 2015;3:2903–13.

[287] Yang S, Wang S, Liu X, Li L. Biomass derived interconnected hierarchical micro-meso-macro- porous carbon with ultrahigh capacitance for supercapacitors. Carbon 2019;147:540–9.

[288] Gu X, Wang Y, Lai C, Qiu J, Li S, Hou Y, et al. Microporous bamboo biochar for lithium-sulfur batteries. Nano Res 2015;8:129–39.

[289] Sevilla M, Mokaya R. Energy storage applications of activated carbons: supercapacitors and hydrogen storage. Energy Environ Sci 2014;7:1250–80.

[290] Hu S, Zhang S, Pan N, Hsieh Y-L. High energy density supercapacitors from lignin derived submicron activated carbon fibers in aqueous electrolytes. J Power Sources 2014;270:106–12.

[291] Goldfarb JL, Dou G, Salari M, Grinstaff MW. Biomass-based fuels and activated carbon electrode materials: an integrated approach to green energy systems. ACS Sustainable Chem Eng 2017;5:3046–54.

[292] Sun T, Levin BDA, Guzman JJL, Enders A, Muller DA, Angenent LT, et al. Rapid electron transfer by the carbon matrix in natural pyrogenic carbon. Nat Commun 2017;8:14873.

[293] Qian T, Yang Q, Jun DCF, Dong F, Zhou Y. Transformation of phosphorus in sewage sludge biochar mediated by a phosphate-solubilizing microorganism. Chem Eng J 2019;359:1573–80.

[294] Zhu X, Chen B, Zhu L, Xing B. Effects and mechanisms of biochar-microbe interactions in soil improvement and pollution remediation: a review. Environ Pollut 2017;227:98–115.

[295] Chen S, Rotaru A-E, Shrestha PM, Malvankar NS, Liu F, Fan W, et al. Promoting interspecies electron transfer with biochar. Sci Rep 2014;4:5019.

[296] Wang C, Liu Y, Gao X, Chen H, Xu X, Zhu L. Role of biochar in the granulation of anaerobic sludge and improvement of electron transfer characteristics. Bioresour Technol 2018;268:28–35.

[297] Liu B, Ren W, Gao L, Li S, Pei S, Liu C, et al. Metal-catalyst-free growth of single-walled carbon nanotubes. J Am Chem Soc 2009;131:2082–3.

[298] Chen W, Li Y, Zhu D, Zheng S, Chen W. Dehydrochlorination of activated carbon-bound 1,1,2,2-tetrachloroethane: implications for carbonaceous material-based soil/sediment remediation. Carbon 2014;78:578–88.

[299] Liu L, Yang X, Hou Q, Zhang S, Ju M. Corn stalk conversion into 5-hydroxymethylfurfural by modified biochar catalysis in a multi-functional solvent. J Clean Prod 2018;187:380–9.

[300] Sun X, Atiyeh HK, Li M, Chen Y. Biochar facilitated bioprocessing and biorefinery for productions of biofuel and chemicals: a review. Bioresour Technol 2020;295:122252.

[301] Rafi JM, Rajashekar A, Srinivas M, Rao BVSK, Prasad RBN, Lingaiah N. Esterification of glycerol over a solid acid biochar catalyst derived from waste biomass. RSC Adv 2015;5:44550–6.

[302] Hidayat A, Rochmadi R, Wijaya K, Budiman A. Reaction kinetics of free fatty acids esterification in palm fatty acid distillate using coconut shell biochar sulfonated catalyst. 2015.

[303] Akinfalabi S-I, Rashid U, Yunus R, Taufiq-Yap Y. Appraisal of sulphonation processes to synthesize palm waste biochar catalysts for the esterification of palm fatty acid distillate. Catal 2019;9:184.

[304] Ormsby R, Kastner JR, Miller J. Hemicellulose hydrolysis using solid acid catalysts generated from biochar. Catal Today 2012;190:89–97.

[305] Xiong X, Yu IKM, Chen SS, Tsang DCW, Cao L, Song H, et al. Sulfonated biochar as acid catalyst for sugar hydrolysis and dehydration. Catal Today 2018;314:52–61.

[306] Liang F, Song Y, Huang C, Zhang J, Chen B. Preparation and performance evaluation of a lignin-based solid acid from acid hydrolysis lignin. Catal Commun 2013;40:93–7.

[307] Chen W, Zhu D, Zheng S, Chen W. Catalytic effects of functionalized carbon nanotubes on dehydrochlorination of 1,1,2,2-tetrachloroethane. Environ Sci Technol 2014;48:3856–63.

[308] Fang G, Zhu C, Dionysiou DD, Gao J, Zhou D. Mechanism of hydroxyl radical generation from biochar suspensions: implications to diethyl phthalate degradation. Bioresour Technol 2015;176:210–7.

[309] Mao JD, Johnson RL, Lehmann J, Olk DC, Neves EG, Thompson ML, et al. Abundant and stable char residues in soils: implications for soil fertility and carbon sequestration. Environ Sci Technol 2012;46:9571–6.

[310] Zhang C, Tian S, Qin F, Yu Y, Huang D, Duan A, et al. Catalyst-free activation of permanganate under visible light irradiation for sulfamethazine degradation: experiments and theoretical calculation. Water Res 2021;194:116915.

[311] Fang G, Liu C, Wang Y, Dionysiou DD, Zhou D. Photogeneration of reactive oxygen species from biochar suspension for diethyl phthalate degradation. Appl Catal, B 2017;214:34–45.

[312] Yang J, Pignatello JJ, Pan B, Xing B. Degradation of p-nitrophenol by lignin and cellulose chars: H$_2$O$_2$-mediated reaction and direct reaction with the char. Environ Sci Technol 2017;51:8972–80.

[313] Rubeena KK, Hari Prasad Reddy P, Laiju AR, Nidheesh PV. Iron impregnated biochars as heterogeneous Fenton catalyst for the degradation of acid red 1 dye. J Environ Manag 2018;226:320–8.

[314] Qin F, Peng Y, Song G, Fang Q, Wang R, Zhang C, et al. Degradation of sulfamethazine by biochar-supported bimetallic oxide/persulfate system in

natural water: performance and reaction mechanism. J Hazard Mater 2020;398: 122816.

[315] Cao H, Xing L, Wu G, Xie Y, Shi S, Zhang Y, et al. Promoting effect of nitration modification on activated carbon in the catalytic ozonation of oxalic acid. Appl Catal, B 2014;146:169–76.

[316] Moussavi G, Khosravi R. Preparation and characterization of a biochar from pistachio hull biomass and its catalytic potential for ozonation of water recalcitrant contaminants. Bioresour Technol 2012;119:66–71.

[317] Liu Y, Chen C, Duan X, Wang S, Wang Y. Carbocatalytic ozonation toward advanced water purification. J Mater Chem 2021;9:18994–9024.